DOI: https://doi.org/10.24297/jap.v23i.9747

Prototyping studies for self-sufficient power machines with local resources from the Moon

Ramon Ferreiro Garcia

Former, Prof. Emeritus at the University of A Coruna, Spain

https://www.udc.es , ramon.ferreiro@udc.es

Abstract;

This paper investigates the design challenges of implementing Self-Sustaining Power Machines (SSPMs) for lunar environments using in-situ resources. These machines are engineered to provide on-site energy in the form of heat, mechanical work, or electrical power as required for lunar operations. Given that SSPMs rely on a thermal working fluid for functionality, a key aspect of the design process involves the selection and optimization of this fluid.

Lunar regolith contains trapped gases that can be extracted and utilized—an approach known as In-Situ Resource Utilization (ISRU). Among the available candidate gases (helium, argon, and neon), this study evaluates two SSPM designs compatible with these fluids. These innovative prototypes employ cutting-edge technologies to generate mechanical work through pulling forces, achieved via cooling rather than conventional heating. Notably, the system recovers and regenerates waste cooling heat, enabling reuse without external energy input.

The proposed design framework incorporates a combined cycle (CC) integrating a reverse Brayton cycle (RBC)-based heat pump with an SSPM composed of cascaded power units (PUs). The CC prototype (RBC + SSPM) was tested using helium, argon, and neon obtained through ISRU. Results (Tables 27 and 28) demonstrate that the SSPM-based CC, configured with six PUs operating in a VsVs cycle, achieves a self-sufficient net work output at viable efficiency levels

Keywords: Self heat source, Self-Sustaining Power Machines, Self-heat Power Supply, In-situ resource utilization (ISRU), Moon surface resources and ISRU from Lunar Regolith.

Nomenclature related to general VsVs cycles and SSPMs

Acronyms	**Description/Context**
Exp.	Expansion process: A form of expansion (volume increase) achieved by heating a TWF, which generates a **push** force while decreasing internal energy and pressure.
Cont.	Contraction process: A form of compression (volume reduction) previously achieved by cooling a TWF, which generates a **pull** force giving rise to output useful work.
Comp.	Compression process: A form of compression (volume reduction) achieved by adding useful work to the system by means of a **push** force, resulting in increased pressure and internal energy.
Suct.	Suction process: A form of expansion (volume increase) achieved by adding useful work to the system by means of a **pull** force, while decreasing internal energy and pressure.
CTF	Cooling Transfer Fluid (conventionally, thermal oil)
EM	electromagnetic
EP	Electric Power
FCF	Forced convection fan (recirculation fan of the TWF)
FP	Feed pump (feed compressor of the TWF)
G	Electric Power Generator: alternator or generator
HTF	Heating Transfer Fluid (conventionally, thermal oil)
Is_eff	Isentropic efficiency: (open processes). A coefficient of losses inherent to real gas expansion or compression
MT	Metric Tons: a metric Ton = 1000 kg
LF	Losses factor (include thermo-mechanical and thermo-hydraulic losses)
PP	Power Plant: a set of cascaded PUs or a combined cycle based on cascaded PUs and a RBC
PU	Power Unit operating with the thermal cycle such as the VsVs cycle

RF	Losses factor dealing with heat recovery factor (includes heat transfer losses and leaks)
RIT	Ratio of Isochoric low to high temperatures [T_L/T_H], [T_1/T_3] for sVsVs, and [T_1/T_2] for VsVs,
SSI	Self-Sustaining Index: means the net gained energy as % : [$SSI = (\eta_{th} - 100)/100$]
SSHS	Self-Sustaining Heat Supply
SEP	Self-Electric Power: SEP ≈ SSI (net mechanical power ≈ net electrical power)
sp	State point of any stationary point state of a thermal cycle
SSPM	Self-Sustaining Power Machine, Self-Sufficient Power Machine
SSPP	Self-Sustaining Power Plant, Self-Sufficient Power Plant
sVsVs	Cycle with the sequential processes: [isentropic-adiabatic (s), Isochoric (V), s,V,s]
TWF	Thermal Working Fluid (thermal working fluid subjected to heat-work interactions carried out in the machine or system considered).
VsVs	Cycle with the sequential processes: [isochoric (V), isentropic-adiabatic (s), V, s]
CC	Combine Cycle
RBC	Reversed Brayton Cycle
FLT,	First law of thermodynamics
SLT,	Second law of thermodynamics
SHS	Self heat source
SHSk	Self heat sink
SHPS	Self-self-heat power supply
MAR	Moon atmosphere resources
Symbols/units	***description***
p(bar)	pressure
q_i(kJ/kg)	specific heat in to a cycle process
q_{i23}(kJ/kg)	Input heat to cycle process 2-3
q_o(kJ/kg)	specific heat out from a cycle process
q_{o41}(kJ/kg)	output heat from cycle process 4-1 in a VsVs cycle
q_{rec}	Recovered heat from cycle process 4-1 in a VsVs cycle
Cp(kJ/kg-K)	specific heat capacity at constant pressure
Cv(kJ/kg-K)	specific heat capacity at constant volume
s(kJ/kg-K)	specific entropy
h(kJ/kg)	specific enthalpy
T(K)	temperature
T_H(K)	top cycle temperature
T_L(K)	bottoming cycle temperature
u(kJ/kg)	specific internal energy
v(m^3/kg)	specific volume
V(m^3)	volume
w(kJ/kg)	specific work
w_i(kJ/kg)	specific work input
w_{iFP}(kJ/kg)	Work added to drive the feed pump responsible to transfer the TWF

w_o(kJ/kg)	specific work out
w_{oexp} (kJ/kg)	Output expansion work due to previously added heat
w_{ocont} (kJ/kg)	Output contraction work due to previously extracted heat
w_{oexp23} (kJ/kg)	Output expansion work w_{o23} due to previously added heat
$w_{ocont41}$ (kJ/kg)	Output contraction work w_{o41} due to previously extracted heat
w_n (kJ/kg)	Net useful work ($w_{oexp} + w_{ocont}$) = ($w_{o23} + w_{o41}$)
wnT (kJ/kg)	Total net work (RBC work + Cascaded VsVs cycles works)
q_{rec}/PUi[kJ/kg]	Heat recovered from every PU from cooling cycles processes
T_{q_rec}/PUi [K]	Temperature of the heat recovered from cooling cycles processes in every PU
η_{th} (%)	Cycle thermal efficiency [w_n/qi]

Nomenclature related to Moon data, characteristics and necessary activities

Acronym	Full Form	Description/Context
RDAC	Reciprocating Double-Acting Cylinder	A type of actuator used in thermal machines for contraction-based work.
ISRU	In-Situ Resource Utilization	The practice of collecting and processing local resources (e.g., He-3, Ar, Ne, water) for fuel, life support, and construction.
PSA	Pressure Swing Adsorption	A gas separation technique that uses pressure changes to adsorb/desorb gases (e.g., CO_2 capture).
ESA	European Space Agency	The European counterpart to NASA, involved in Moon exploration research.
AI	Artificial Intelligence	Used for data approximation (e.g., Moon atmospheric composition).
RBC	Reversed Brayton Cycle	Used as heat pump enabled to transfer heat from a cool heat sink to a Ho heat source
CCs	Combined Cycles	In this work is a combination of thermal cycles: RBC and SSPM,
RBS-SSPM	a combination between a RBC and SSPM cycles	a RBC operating as power source and sink, while SSPM use it as power source and sink.

1 Introduction

The Moon's Role as a Critical Hub for Space Exploration and Resource Utilization

The Moon is a crucial intermediate station between Earth and other planets in the solar system, as well as a gateway to deeper space. For this reason, the exploration and utilization of lunar resources are essential—both for advancing in-situ resource utilization (ISRU) technologies and addressing resource scarcity on Earth.

However, extracting and processing the Moon's natural resources demands significant energy inputs, including electrical power, heat, and mechanical work. Given that sufficient electrical energy can also provide heat and mechanical work through conversion, the key challenge lies in generating enough power to sustain these operations.

The Moon's regolith—a surface layer approximately three meters thick—contains fundamental resources for power generation, including helium, argon, and neon, which can serve as efficient thermal working fluids in energy cycles. Traditional power generation methods (such as solar thermal, photovoltaic, and nuclear fission or future fusion reactors) face limitations in this environment. In contrast, the Self-Sustaining Power Machines (SSPMs) proposed in this study offer a more advantageous solution.

SSPMs are fully autonomous, requiring no external input to operate the machines or services they support. This study focuses on their design, prototyping, and potential applications in the lunar environment, presenting a sustainable approach to powering lunar exploration and resource exploitation.

To explore, exploit, and transform or manufacture a habitable environment for Moon resources, both those of its soil and subsurface mineral resources [1-5], a production structure based on automated, self-sufficient, and/or autonomous manufacturing processes that require significant electrical power consumption is

required. Likewise, environments adapted to plant and animal life must be protected from both solar and cosmic radiation [6-7], which entails significant electric power consumption.

Some of the most common intensive electricity consumers include:

Reusable Rockets for landing and takeoff using low-cost compressed and further reheated liquid as propulsion fluids by means of in-situ (on board) by means of electrical techniques including magnetic induction and microwaves. Mainly for low-orbit takeoff,

Light helicopters and drones,

Autonomous transport vehicles, cranes, tracks, minerals-processing tools,

Drilling machines, excavators, tunnel boring machines, or backhoe loaders,

Casting of ferromagnetic metals and alloys,

Manufacture of utensils and tools with ferromagnetic materials,

Brick firing phase for the construction of anti-radiation barriers and habitats equipped with artificial light and all necessary services.

Therefore, given the recognized need to produce as much electrical energy as necessary autonomously, disruptive, viable and breakthrough technical solutions are proposed, without which any attempt to colonize Moon would de facto represent a major failure for the human being.

So, given the meteorological conditions on Moon, characterized by an average minimum temperature below that of Earth, we are enabled to provide a heat sink that significantly aids the production of electrical energy. Even using this advantage, we still face the challenge of producing electrical energy without using heat sources and a heat sink.

This work must address three disruptive technological challenges to enable the implementation of efficient PUs equipped with the capability to operate through heat-work interactions based on vacuum thermal contraction achieved through cooling with heat extraction in closed adiabatic processes, as described in [8-10]. The first challenge is that the proposed heat engine prototype must be capable of supporting V/V thermal cycles. The second challenge is that the thermal cycles must be able to release cooling heat for efficient recovery upstream.

The third challenge involves feasible and highly effective forced convection heat transfer techniques to provide both heat addition and extraction for the minimum physically feasible time in each PU, where each PU is composed of a pair of Double-Acting Reciprocating Actuators (DARAs) equipped with their respective associated heat transfer systems. Likewise, the combination of two conversion techniques already published [11-14] and [16-19] allow contributions to the operation of plants capable of operating without an external heat source or heat sink, which consist of combined cycles between SSPMs formed by PUs in cascade and a heat pump formed by the RBC thermal cycle. Studies have been carried out for the design and prototyping of these power plants using real gases as working fluids, with data obtained from E. W. Lemmon et al. [15]. The case study is focused on improving the performance of SSPMs through disruptive thermal regeneration techniques in the power units (PU), using upstream cascade heat recovery to achieve high performance rates overcoming the drawbacks of being subject to the existence of gases as thermal working fluids (TWF) available on-site. The prototyping tasks for the studied cases are covered by patents referenced in [20-22].

Since the objective of this work is solely the supply of energy under quality conditions, both ambient and on demand, to address the performance of all necessary tasks in situ, both in the lunar environment and on aerospace transport routes, Section 2 briefly describes the physical, chemical, and environmental conditions of the lunar environment. Section 3 addresses the actuator systems responsible for mechanical work, which constitute a significant part of the PUs. Section 4 addresses practical cases to validate the design and implementation of potential prototypes. Section 5 analyzes and discusses the results; and Section 6 draws some conclusions that provide clarity and a vision for the future of the sustainable model proposed in this work.

2. Essential Resources and Weather on the Moon

Understanding lunar resources and environmental conditions is vital for sustaining human exploration, enabling mining operations, and establishing the Moon as a staging point for Moon missions. This knowledge also informs broader strategies for extracting non-renewable resources across the solar system using autonomous technologies. Therefore, it is of great importance to have the necessary elements to operate in each and every one of the processes carried out for resource exploration. Among these resources, energy resources occupy the first place; that is, those without which it is not possible to generate sufficient electrical energy to carry out the extraction and exploitation tasks. In this regard, it is worth noting that the main gases that can be exploited are

fortunately helium, argon, and neon, which are necessary and indispensable for operating electricity-producing machines equipped with technology that makes them self-sufficient.

2.1 Lunar Weather (AI-Assisted Analysis)

Reference: [18] NASA – Weather on the Moon. (https://science.nasa.gov/moon/weather-on-the-moon/)

1. No Atmosphere: The Moon's exosphere is negligible (near-vacuum), eliminating weather phenomena like wind or precipitation.

2. Extreme Temperatures:

--Daytime (Sunlit Side): Up to 127°C

--Nighttime (Dark Side): As low as -173°C

--Rapid swings occur due to lack of atmospheric insulation.

3. Radiation & Micrometeoroids: Unfiltered solar radiation and frequent micrometeorite impacts (no atmospheric protection).

4. Surface Preservation: No erosion or weathering; geological features remain unchanged except by meteor impacts.

5. Dust Dynamics: Electrostatic forces levitate dust, creating faint "storms" near the day-night boundary.

Summary: The Moon has no traditional weather—only temperature extremes, radiation, and electrostatic dust activity.

2.2 In-Situ Resource Utilization (ISRU) on the Moon

The Moon has virtually no atmosphere. In other words, the amount of recoverable gases is reduced to trace amounts, making the exploitation of such resources unviable. Instead, the hope is to explore and exploit the resources contained in the regolith in a layer of the lunar surface up to about three meters deep. In addition to regolith, other mining resources are expected to be processed, all of which require a robotic industry for extraction and processing with intensive consumption of energy produced on-site.

2.2.1 Exosphere Resources (Trace Gases**)**

The lunar exosphere contains negligible but strategically interesting elements:

--Helium-3 (^3He): Potential fusion fuel (solar wind-deposited).

--Hydrogen (H_2): Feedstock for water synthesis.

--Trace Elements: Neon (Ne), argon (Ar), sodium (Na), potassium (K) (non-recoverable at scale).

Table 1 depicts a list of the lunar significant components of the exosphere necessary to be used as TWFs.

Table 1: Potential (traces) of useful gases as TWF for SSPMs on Lunar exosphere composition

Element	**Concentration (atoms/cm^3)**	**Potential in-situ applicableness**
Helium (He)	5,000–30,000	Future fusion reactors, TWF for SSPMs
Argon (Ar	20,000–100,000	TWF for SSPMs
Neon (Ne)	< 20,000	TWF for SSPMs

Summarizing, exosphere resources are impractical for extraction. As consequence, He, Argon and Neon must be obtained from the regolith existing on the Moon surface.

2.2.2 Surface Resources (Regolith)

Since the propulsive power of rockets capable of landing on the lunar surface as well as take-off depends essentially on the gases required by the propulsion system to operate, it is important to discuss the thermal working fluids used in such systems. These demanded gases are classified into two categories:

1 gases used in propulsion to produce thrust by reaction, and

2 These gases are required as thermal working fluids in SSPMs, responsible for producing the electrical energy needed to heat the propellant gases and generate sufficient thrust. Hence the importance of exploring and exploiting the lunar surface regolith to obtain abundant quantities of these gases.

Fortunately, lunar regolith contains trace amounts of helium (He), argon (Ar), and neon (Ne), which are implanted by the solar wind over billions of years. Here's a breakdown of their presence:

-- **Helium-3 (^{3}He).** Source: Solar wind implantation (not primordial).

Significance: Helium-3 is rare on Earth but relatively more abundant on the Moon. It is considered a potential fuel for future nuclear fusion reactors. However it is also useful as TWF on SSPMs.

Concentration: Estimated at 1–50 parts per billion (ppb) in the regolith, depending on location.

-- **Neon (Ne).** Source: Solar wind (like helium).

Presence: Found in lunar soil samples (e.g., Apollo missions).

Concentration: Around 10–20 parts per million (ppm) in some samples.

-- **Argon (Ar).** Sources: Solar wind (Ar-36, Ar-38)

Radiogenic decay of potassium-40 (Ar-40) from lunar interior outgassing.

Presence: Detected in lunar regolith, with Ar-40 being more abundant due to potassium decay.

Concentration: Varies, but Ar-40 can be tens of ppm in some soils.

As key observations it can be highlighted that these gases are trapped in the glassy surfaces of regolith grains due to solar wind bombardment.

Older regolith (exposed longer to solar wind) tends to have higher concentrations.

Cold traps near lunar poles may retain more volatile gases.

Apollo Mission Findings: Apollo samples confirmed the presence of He, Ne, and Ar.

Lunar atmosphere has trace amounts of these gases, but they are extremely tenuous.

Future Implications: Helium-3 mining has been proposed as a long-term goal for lunar resource utilization.

Neon and argon could be useful for life support or industrial processes in future lunar bases.

The lunar surface layer reaches a thickness of about 3 m. This suggests that there is a significant amount of useful elements that can be explored and exploited.

In addition to the gases mentioned above that are especially useful for use as TWFs, Table 2 shows other high-value regolith components for in-situ use.

Table 2: A list of the Key Regolith Components on Moon surface

Resource	Use Case
Oxygen	Extracted via electrolysis (40–45% of regolith by weight
Metals: (Si, Al, Fe, Ti)	Construction, manufacturing
Helium-3 (^{3}He)	Fusion fuel (1–20 ppb in soil
Water Ice	Polar craters (1.6B+ metric tons estimated

2.2.3 Additional Critical Resources:

-- **Water Ice:** Found in permanently shadowed polar craters (e.g., Shackleton Crater). Supports life and fuel production (H_2/O_2) also used for conventional propulsion.

-- **Solar Energy**: Near-constant sunlight at poles (ideal for solar farms).

Moon Minerals: Uses and Potential Applications

The following minerals listed in Table 3—silica (SiO_2), alumina (Al_2O_3), lime (CaO), and iron(II) oxide (FeO)—are abundant on the Moon and have significant potential for future lunar exploration and colonization. Let's consider how they might be used:

Table 3: A list of the major components of lunar soil, including regolith, from which helium, argon, and neon are extracted.

Compound	**symbol**	**Maria (%)**	**Highlands (%)**	**Main utilities**
silica	SiO_2	45.4%	45.5%	Glass & Solar Panels, Fiber Optics & Electronics, Ceramics & Construction and Oxygen Production:

alumina	Al_2O_3	14.9%	24.0%	Aluminum Production, Ceramics & Insulation, Abrasive & Protective Coatings, Transparent Armor:
lime	CaO	11.8%	15.9%	Cement & Concrete, Soil Stabilization**,** Oxygen Production
iron(II) oxide	FeO	14.1%	5.9%	Iron & Steel Production, Radiation Shielding, Thermal Storage, Oxygen Production:

Silica (SiO_2)

--Glass & Solar Panels: Silica is a primary component in glass manufacturing, which can be used for windows, solar panels, and protective coatings.

--Fiber Optics & Electronics**:** High-purity silica is essential for fiber-optic cables and semiconductor devices.

--Ceramics & Construction: Can be used to make heat-resistant tiles, bricks, and other structural materials.

--Oxygen Production: Can be processed to extract oxygen (via reduction with hydrogen or electrolysis).

Alumina (Al_2O_3)

--Aluminum Production: A key source of aluminum, which is useful for spacecraft, habitats, and machinery.

--Ceramics & Insulation: Used in high-strength, heat-resistant ceramics for habitats and industrial applications.

--Abrasive & Protective Coatings: Useful for manufacturing tools and wear-resistant surfaces.

--Transparent Armor: Aluminum oxynitride (a derivative) can be used for strong, transparent windows.

Lime (CaO)

--Cement & Concrete**:** Mixed with lunar regolith, it can help produce concrete for construction.

--Soil Stabilization**:** Helps bind loose regolith for roads and landing pads.

--Oxygen Production**:** Can be processed to release oxygen (via thermal decomposition or chemical reactions).

--**Water Purification & pH Control**: Useful in life-support systems for managing water quality.

4. Iron(II) Oxide (FeO)

--Iron & Steel Production: Can be reduced to extract metallic iron for construction and machinery.

--Radiation Shielding: Iron-rich materials can be used in habitats to block cosmic rays.

--Thermal Storage: Iron oxides can store heat in thermal energy systems.

--Oxygen Production: When reduced, FeO releases oxygen (e.g., via hydrogen reduction: $FeO + H_2 \rightarrow Fe + H_2O \rightarrow$ electrolysis $\rightarrow O_2$).

Additional Benefits:

--(ISRU): These minerals reduce the need to transport materials from Earth, lowering mission costs.

--Oxygen for Life Support & Fuel**:** Many of these oxides can be processed to extract breathable oxygen or rocket propellant (LOX).

--3D Printing & Additive Manufacturing**:** Lunar regolith (containing these minerals) can be used in 3D-printed structures.

2.3 Estimated Lunar Resource Quantities

Water Ice:

-- Polar Regions: ~1.6B metric tons (LCROSS mission).

-- Shackleton Crater:Up to 600M metric tons (5–10% regolith mass).

Helium-3:

-- Concentration: 0.01–0.1 g/ton of soil.

-- Total Reserves: ~1.1M metric tons (theoretical).

Metals (per ton of regolith):

--Silicon (20%), Aluminum (10–15%), Iron (5–15%).

Key Takeaway: Water and ^{3}He are top-priority resources; metals require **energy-intensive** processing. However, the demand of electrical/heat energy is successfully solver by means of Self-sustaining Power Machines.

2.4 Strategic Exploitation Plans

Mining Initiatives:

--Water Ice: Astrolab's FLIP rover joins Astrobotic's Griffin-1 to the Moon).

https://www.astrobotic.com/astrolabs-flip-rover-joins-astrobotics-griffin-1-to-the-moon/

--Metals: ESA's PROSPECT mission.

--Helium-3: China's Chang'e missions, Moon Express.

The data in Table 4 give a precise idea of the large amount of energy required for extraction, processing and exploitation operations to carry out operations even under habitable conditions. It is shown that to obtaining a kg of Helium-3 requires processing an amount of regolith that approaches 150000 tones. This operation

ISRU Technologies

-- Oxygen Production: NASA's ROxygen project (electrolysis of regolith).

-- Habitat Construction: 3D-printed regolith structures (ESA's LUNA facility).

Legal Frameworks

-- Artemis Accords: Governance for lunar mining.

-- Commercial Players: Blue Origin (Blue Alchemist), SpaceX (Starship cargo).

2.5 Justification for Lunar Helium-3 Exploitation

Applications of ^{3}He:

1. Nuclear Fusion: Aneutronic reaction with deuterium (minimal radioactive waste).

2. Neutron Detection: Critical for nuclear security.

3. Cryogenics: Enables near-absolute-zero temperatures (quantum computing).

4. Medical Imaging: Lung MRI (hyperpolarized ^{3}He).

Challenges:

-- Scarcity: Rare on Earth; lunar reserves require massive processing.

-- Energy Demand: Mining 1g ^{3}He needs 150 tons of regolith.

Future Outlook: Solar-Shielded Power Modules could enable extraction using in-situ working fluids (e.g., helium-4, argon, neon). These fluids are excellent gases to be used as thermal working fluids (TWFs) necessary to operate Self-Sustaining Power Machines (SSPMs), which would supply the electrical energy required for all operations carried out in the massive extraction of resource processing and exploitation.

The widespread adoption of SSPMs enables full industrialization, capable of meeting any energy demand without relying on fusion reactors for electricity generation. Additionally, each material extraction and processing machine is integrated directly into the architecture of the SSPM itself.

The following section addresses the problem of the preliminary design of prototypes of self-sufficient machines operating with Helium, Argon or Neon, which enables them to overcome the advantages of nuclear fusion reactors. These disruptive technology breakthroughs also pave the way to explore at least the rest of the Solar System.

3 The behavior of forces exerted on or by a single or double-acting thermo mechanical actuators

This section concerns the VsVs thermal cycle used in PUs corresponding to Self-Sustaining Power Machines (SSPMs). The operating principles are described, subject to heat-work interactions by thermal contraction, which

are not considered in energy balances assumed by the first law of thermodynamics (FLT), which is why it exhibits a flagrant controversy.

In order to investigate the causes that give rise to thermal cycles enabled to do mechanical useful work using a strategy based on extracting heat from TWFs without energetic costs, let's begin this section studying the behavior of forces exerted on or by a Single-Acting Reciprocating Actuator (SARA).

Taking into consideration the thermodynamic and dynamic behavior of a single-acting linear actuator, which consists of a single-acting reciprocating cylinder, it is experimentally observed that the interactions between the force generated in its actuation chamber (AC) and the force and motion transmitting mechanism (rod-piston) obey the behavior bellow described. In Fig. 1 the meaning of used notation is as follows: P_A, F_A: pressure and force into actuator chamber, Ps, Fs: Surroundings pressure and force. Therefore, considering the thermodynamic and dynamic behavior of a Single-Acting Reciprocating Actuator (SARA), which consists of a single-acting reciprocating cylinder, it is experimentally observed that the interactions between the force generated in its AC and the force and motion transmitting mechanism (rod-piston) obey the following behavior:

Assuming that the meaning of expansion and compression is well known, let us define two variants that need to be understood precisely:

--Suction (volume increase) is a form of **expansion** (resulting in decreased temperature and pressure) where **work is done on the system** rather than extracted from it: **Useful work is added while internal energy decreases which is not consistent when compared with Eqs. (1) and (2) of the FLT**

--Contraction (volume decrease) is a form of **compression** (resulting in increased temperature and pressure) where **work is extracted from the system** rather than applied to it: **Useful work is obtained while internal energy increases which is not consistent when compared with Eqs. (1) and (2) of the FLT**

Fig. 1 illustrates the possible dynamic cases of interactions between mechanical and thermal magnitudes. Among mechanical magnitudes are inward-outward forces, linear movement and useful mechanical work.

Among thermal magnitudes are internal (force-motion-work) interactions carried out by experimental tests. The first observations yield obvious results which include:

--Input forces (such as compression or suction) exerted on the thermal working fluid of the actuator are generated by an external mechanical action through the piston-rod.

--Output forces exerted by a thermal working fluid on the piston-rod (such as expansion or contraction) are transferred to the surroundings as useful work

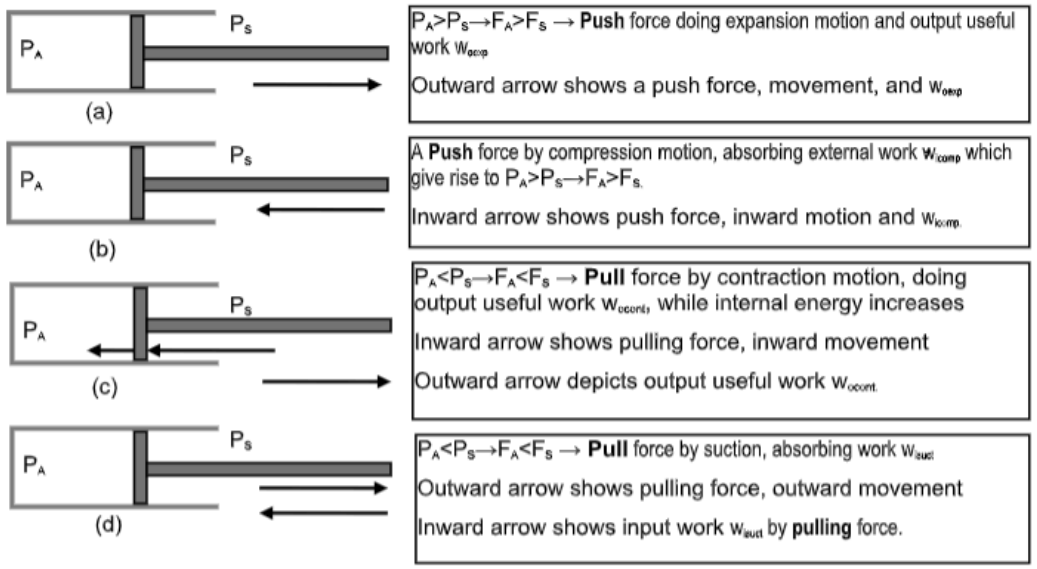

Figure 1: Experimental validation of the Heat-work interactions that exhibit input suction work and/or Output contraction work, both involving pulling forces

This section attempts to introduce the controversial idea that all energy entering a closed process through a heat-work interaction contributes to increasing its internal energy, and all energy leaving a closed process through a heat-work interaction contributes to decreasing its internal energy.

However, evidence based on experimental observation will demonstrate that this assertion, reinforced by the first law of thermodynamics, is partially true; that is, it is not general. Among the four existing types of forces, there are two unusual forces that do not obey this principle. Therefore, this phenomenon can only be resolved by considering it in energy balances based on the results of experimental observations.

Thus, given the relevance of such unusual forces in thermal cycles that perform useful mechanical work through thermal contraction, and that give rise to thermal cycles with unprecedented efficiencies, it is necessary to understand the reasons for this controversy.

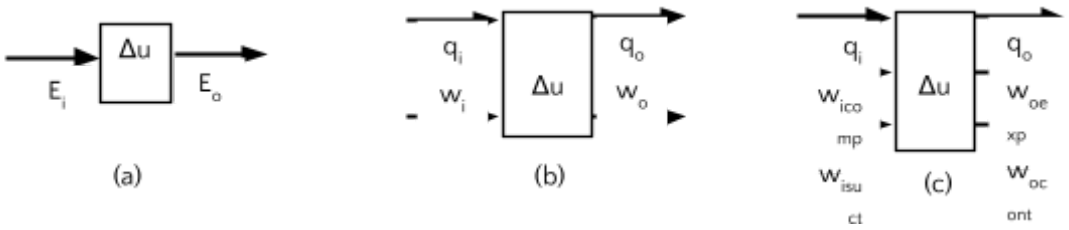

Figure 2: Thermodynamic models of heat-work interactions — heat-force/motion/work interactions— based on FLT

In Fig. 2 it is depicted three block diagrams illustrating the same meaning: Both are similar in terms of energy balance (a) = (b) = (c). However the energy balance in (c) fails because it contains two interactions w_{isuct} and w_{ocont} which do not satisfy such an energy conservation theorem based on the first principle or principle of conservation of energy.

Fig. 2, illustrates how according to the FLT all input magnitudes contribute to increasing internal energy.

However, according to experimental observations input suction work (w_{isuct}) and output contraction work (w_{ocont}) do not obey such fundamental statement.

Table 1: Possible forces exerted on/by a SARA and observed results **(inconsistent with FLT but True)**

Causal magnitudes	**Observed results on energy balance consistence with FLT**			
	Observed push forces: consistent		**Observed pull forces: inconsistent**	
Causal action: mechanical	**Input** Compression force F_{icomp}	**+Δu**	**Input** Suction force F_{isuct}	**—Δu**
Causal action: thermal	**Output** Expansion force F_{oexp}	—Δu	**Output** Contraction force F_{ocont}	**+Δu**

Table 1 illustrates that:

--according to the FLT all input magnitudes contribute to increasing internal energy

--according to observation input suction work (w_{isuct}) and output contraction work (w_{ocont}) do not obey FLT.

In order to obey FLT, the results should be as depicted in the Table 2. However, such predicted results obeying FLT are highlighted in red color are false.

Table 2: Possible forces exerted on/by a SARA and predicted results by **FLT (consistent with FLT but False)**

Causal magnitudes	**Prediction results from the energy balance based on FLT**			
	Push forces: consistent		**Pull forces: consistent**	
Causal action: mechanical	**Input** Compression force F_{icomp}	**+Δu**	**Input** Suction force F_{isuct}	**+ Δu**
Causal action: thermal	**Output** Expansion force F_{oexp}	—Δu	**Output** Contraction force F_{ocont}	**—Δu**

3.1 Energy Balances in SARAs based on FLT

As illustrated in Fig. 2, the energy balance for closed processes involving heat-work interactions—governed by heat, force-motion-work—can be expressed as follows:

From Fig. 2(a), we derive:

$$E_i - E_o = \Delta u \tag{1}$$

This implies that:

$$q_i + w_i - q_o - w_o = \Delta u \tag{2}$$

Equations (1) and (2), based on the First Law of Thermodynamics (**FLT**), indicate that heat-work interactions in closed processes lead to two key effects:

1. Input energy (q_i and w_i) increases the internal energy of the closed system.
2. Output energy (q_o and w_o) decreases the internal energy of the closed system.

A more detailed energy balance, accounting for suction and contraction work (as shown in Fig. 2(c)), can be described by Eqs. (3) and (4):

$$w_i = w_{icomp} + w_{isuct} \tag{3}$$

$$w_o = w_{o\exp} + w_{ocont} \tag{4}$$

According to Eqs. (3) and (4), the FLT implies:

1. Suction work (input work, w_{isuct}) increases internal energy.
2. Contraction work (output work, w_{ocont}) decreases internal energy.

However, experimental evidence (Fig. 1(c) and (d)) contradicts these FLT-based predictions, challenging the principle of energy conservation when suction and contraction works are involved. Specifically:

1. Input work (**suction**), w_{isuct} **decreases** internal energy, whereas the **FLT predicts an increase**.
2. Output work (**contraction**), w_{ocont} **increases** internal energy, whereas the **FLT predicts a decrease**.

Discussion:

Notably, the **FLT does not explicitly account for traction forces** in **suction and contraction work**. When these forces are included, the energy balance yields:

$$E_i - E_o = q_i + w_{icomp} + w_{isuct} - q_o - w_{o\exp} - w_{ocont} = \Delta u \tag{5}$$

which does not occur in reality and therefore Eq. (5) is false.

The only solution to satisfy the FLT as stated is to eliminate the traction or pulling forces from the equation (5), which leaves:

$$E_i - E_o = q_i + w_{icomp} - q_o - w_{o\exp} = \Delta u \tag{6}$$

This leads to establishing a limit of application of the energy balances based on the FLT:

The balances that include **tensile**, **traction** of **pulling** forces (F_{isuct} and F_{ocont}) do not obey the FLT. These experimental observations (Fig. 1(c) and (d)) challenge the conventional FLT formulation and, consequently, the principle of energy conservation in systems where suction and contraction work are significant is not valid.

The work supplied to a cylinder through its rod to generate suction or vacuum based on the increase in volume and decrease in pressure, contributes to a decrease in internal energy instead of contributing to an increase in internal energy.

This experimental result is inconsistent with FLT. According to FLT, the work supplied to a closed system generating decreasing of temperature (internal energy) and pressure contributes to an increase in its internal energy.

Since the thermal cycles proposed for the implementation of SSPMs are made up of power units whose fundamental part consists of the double-acting reciprocating cylinder (DARC), it is important to study their

thermodynamic behavior in order to understand their practical abilities that allow them to operate not only by adding heat but also by extracting heat as a fundamental part, since their abilities to achieve efficiencies never before obtained are derived from this characteristic.

3.2 Test Bench Based on a DARA for Experimental Validation of Thermodynamic Behavior

The objective of the test bench is to experimentally validate the thermodynamic behavior of a double-acting cylinder subjected to the reciprocating displacement of a piston. The experiment consists of evaluating the thermodynamic operating modes when subjected to a thrust force applied to the piston rod. As a result of the applied force, the piston rod moves along its stroke, returning to its initial position.

As shown in Fig. 3, the piston moves from an intermediate rest position (equilibrium) to a stroke limit and returns to the initial position through applied mechanical work on the piston and rod. The process assumes adiabatic-isentropic heat-work interactions, with work absorbed and released by the system.

Experimental Phases (Refer to Fig. 3):

Table 3: Illustration of the thermodynamic behavior of a double-acting cylinder subjected to reciprocating piston displacement. The piston moves from an intermediate rest position (equilibrium) to a stroke limit and returns to the initial position through applied mechanical work on the piston rod.

CC-**A**-He	T(K)	p(bar)	V(m^3)	u(kJ/kg)	s (kJ/kg. K)	**CC-B-He**	T(K)	p(bar)	V(m^3)	u(kJ/kg)	s (kJ/kg. K)
1	400	10	0.83375	1251.8	24.719	1	400	10	0.83375	1251.8	24.719
2	500	17.477	0.59703	1563.8	24.719	2	338.4	6.583	1.0707	1059.7	24.719
1	400	10	0.83375	1251.8	24.719	1	400	10	0.83375	1251.8	24.719

In Table 3 it is depicted the set of data corresponding to the actions carried out by the cylinder when an external excitation based on a thrust force is applied on its piston rod. Both cylinder chambers (CC) A and B are filled with helium at a temperature of 400 K and a pressure of 10 bars. Therefore, according to the data achieved from Table3 it is possible to obtain the results derived from the computation of shown data.

Table 4 illustrates the thermodynamic behavior of a DARC under external excitation. An input force performs work on the system, displacing the piston and piston rod from an intermediate equilibrium position to a stroke limit before returning to the initial position.

With regard to the behavior results, assuming isentropic and adiabatic reversible processes, the results shown in Table 4 confirm that the work contributed to the double-acting actuator causing compression in chamber A and suction in chamber B is fully recovered since it is returned during the reverse stroke as expansion work of chamber A (as its temperature decreases to its equilibrium value), and contraction work in chamber B (as its temperature increases to its equilibrium value).

Table 4: Illustration of the thermodynamic behavior results of a DARC subjected to an external excitation operating with helium as TWF.

Inward motion			Outward motion		
Closed process	Compression	Suction	Closed process	Expansion	Contraction
Cyl. chambers	CC-A	CC-B	Cyl. chambers	CC-A	CC-B
Work input (kJ/kg)	**312**	**192**	Work output (kJ/kg)	**-312**	**-192**

Therefore, the procedure is as follows:

Phase 1: Application of Inward Mechanical Work (Fig. 3 (a))

An inward force displaces the piston into the cylinder, performing two simultaneous thermodynamic processes:

1-2 Isentropic Compression in CC-A:

The trapped working fluid (TWF) in chamber CC-A undergoes compression, leading to increased temperature, pressure, and internal energy while volume decreases.

2-1 Isentropic Suction in CC-B:

The TWF in chamber CC-B experiences suction, causing a decrease in temperature, pressure, and internal energy as volume increases.

Note: *The work input for suction contributes to the reduction in internal energy.*

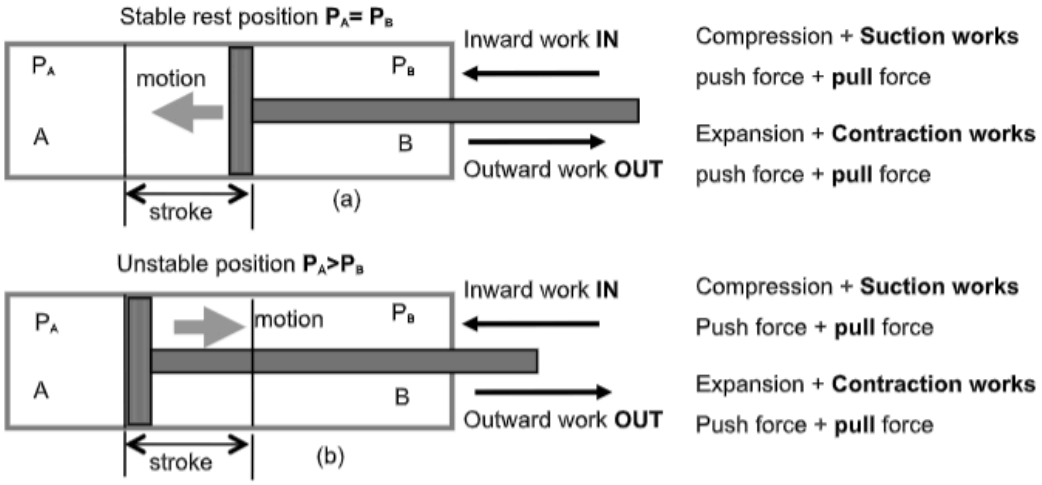

Figure 3: Test bench experiment on a DARC to validate closed adiabatic-isentropic heat-work interactions. (a) Illustrates the intermediate rest position (equilibrium position: $P_A=P_B$). (b) Illustrates the piston rod located at the stroke limit ($P_A>P_B$) ready to return towards its initial or equilibrium position ($P_A=P_B$).

Phase 2: Extraction of Outward Mechanical Work (Fig. 3 (b))

An outward force displaces the piston out of the cylinder, extracting work via two processes:

1-2 Isentropic Expansion in CC-A:

The TWF in CC-A expands, reducing temperature, pressure, and internal energy while volume increases.

2-1 Isentropic Contraction in CC-B:

The TWF in CC-B contracts, increasing temperature, pressure, and internal energy as volume decreases.

Note: *The work output during contraction contributes to the rise in internal energy*

This result contradicts the energy balance applied to closed heat work interactions established by the first principle, which states that according to Fig. 2 (a) and (b) and Eqs. (1) and (2):

Work inputs to a conversion process contribute to an increase in internal energy of a system.

Conversely, work outputs from a conversion process contribute to decrease the internal energy of a system.

In short, the traction (pull or tensile) forces responsible for performing the mechanical work of suction and contraction exert an influence on the energy balances that have profound consequences on the thermal cycles in which they act, since they allow the performance of useful mechanical work without energy cost, as well as a new structure of cascade thermal cycles that give rise to the implementation of self-sufficient power machines based on adequate or effective heat recovery techniques, which with conventional thermal cycles such heat recovery strategies are impossible.

3.3 The heat-work interactions involved in the VsVs thermal cycles

The forces involved in the VsVs thermal cycle as shown in Fig. 4 (a) and (b) are adiabatic expansion (w_{oexp}), (performing useful mechanical work by pushing) and adiabatic contraction (w_{ocont}), (performing useful mechanical work by pulling), where $w_{oexp} = w_{o23}$ and $w_{ocont} = w_{o41}$.

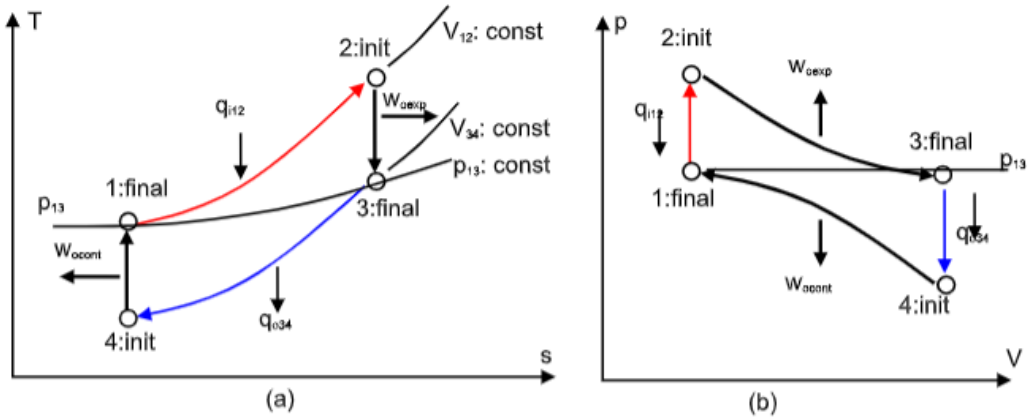

Figure 4: Illustration of force-motion-work interactions in the VsVs cycle based on evidence from experimental validation. The interactions involved in the VsVs cycle are depicted by a T-s diagram in (a) and p-V diagram in (b). Note that the cycle VsVs lack for compression (F_{icomp}) and suction forces (F_{isuct}). Consequently, compression and suction works (w_{icomp}, w_{isuct}) don't exist in this study.

During adiabatic heat-work interactions no heat transfer exist so that $q_i = q_o = 0$. According to Fig. 4 (a) follows thet $q_{i12} = q_{o\,34} = 0$. Therefore assuming that that $w_{icomp} = w_{isuct} = 0$, then follows that according to the FLT:

$-w_{oexp} = \Delta u_{23} = u_{INIT} - u_{FIN} = u_2 - u_3 = Cv.(T_2 - T_3)$: adiabatic expansion **output work** is done while **decreasing** internal energy

And/or

$-w_{ocont} = \Delta u_{41} = u_{INIT} - u_{FIN} = u_4 - u_1 = Cv.(T_1 - T_4)$: adiabatic contraction **output work** is done while **increasing** internal energy

Experimental observations conclude that, according to Table 5, the useful work output is not consistent with the FLT. However, this pull-based force generates useful work output that doubles the total useful work output without adding any thermal energy, although a cooling effect was required without any energy cost. According to the energy balance depicted in Eq. (4) based on observational evidence the total useful work w_{oTOTAL} by cycle and PU is given as:

$$w_{o\,TOTAL} = w_{o\,\exp} + w_{ocont} \tag{7}$$

Table 5: Illustration of the useful mechanical work as a results of two adiabatic heat-work interactions on the cycle VsVs consisting of adiabatic heat addition (q_{i12}) and adiabatic heat extraction (q_{o34}).

Heat-work interaction	**Observed results on energy balance consistence of an VsVs cycle**			
	Observed **push** forces: **consistent**		Observed **pull** forces**: inconsistent**	
Closed adiabatic process	**Output** Expansion force F_{oexp}	**−Δu**	**Output** Contraction force F_{ocont}	**+Δu**

3.4 Cycle transformations for a VsVs discontinuous motion prototype

The proposed thermal cycle for operating SSPMs through cascaded PUs on the lunar surface is illustrated in Fig. 5 (a) and (b). It will be implemented by means of linear actuators based on double-acting reciprocating cylinders (DARCs) as the fundamental pillar of every PU, so that every DARC is considered as the core active component.

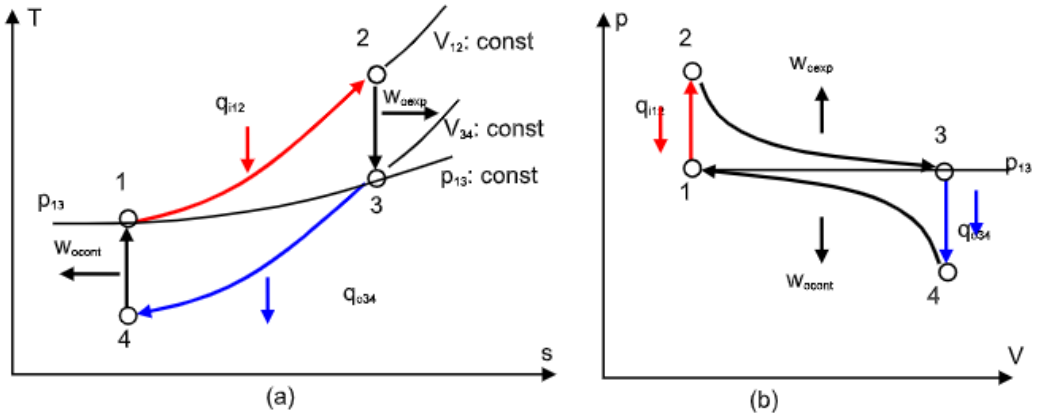

Figure 5: Illustration of a closed processes-based thermal cycle of the type single VsVs. (a): T-s diagram. (b): p-V diagram. The SSPMs operates with cascaded PUs driven by these thermal cycles.

The thermal working fluid is an important part of the SSPM. Such a Power plant is characterized by not requiring any energy from the sun or any other star. It only requires a thermal working fluid (a gaseous chemical compound) that has a lifespan marked by its resistance to deterioration, since it is not consumed but deteriorates and must be regenerated or replaced.

With regard to the information provided in Table 2 and Fig. 2(a), (b), and Figure 5 the thermodynamic transformations between each pair of state points of the cycle carried out on the left side of the discontinuous RDAC are summarized as follows:

Process (1)-(2) corresponds to a closed isochoric heat addition process in which the TWF is heated according to the heat transfer model:

$$q_{i12} = \Delta u_{12} = u_2 - u_1 = Cv \cdot (T_2 - T_1) \tag{8}$$

Process (2)-(3) corresponds to a closed adiabatic expansion process (cylinder chamber volume increases doing work). Thus, the thermal energy in the form of internal energy is converted into mechanical work, provided that the piston can move freely to permit the expansion work.

$$w_{o23} = w_{o\exp} = u_2 - u_3 = Cv \cdot (T_2 - T_3) \tag{9}$$

Process (3)-(4) corresponds to a closed isochoric heat extraction process in which the working fluid is cooled without any work being done because of the constant volume process:

$$q_{o34} = \Delta u_{34} = u_3 - u_4 = Cv \cdot (T_3 - T_4) \tag{10}$$

Process (4)-(1) corresponds to a closed adiabatic contraction-based compression process. Thus, the thermal energy in the form of internal energy is converted into mechanical work by contraction (cylinder chamber volume decreases doing work), provided that the piston can move freely to permit the contraction work:

$$|w_{o41}| = |w_{ocont}| = |u_4 - u_1| = Cv \cdot |(T_4 - T_1)| = Cv \cdot |(T_1 - T_4)| \tag{11}$$

Table 6: Cycle transformations carried out in the VsVs cycle showing the thermodynamic functions carried out simultaneously in both RDACs chambers (A) and (B). The table also depicts the useful work, constant parameters and heat transfer direction associated with each transformation according to Equations (12-17).

VsVs Cycle performed: cylinder chamber **A**				**VsVs** Cycle performed: cylinder chamber **B**			
sp	useful work	constant	heat in/out	sp	useful work	constant	heat in/out
1-2	motionless	V	$q_{i12} = \Delta u_{12}$	3'-4'	motionless	V	$q_{o34} = \Delta u_{34}$
2-3	$w_{o23} = \Delta u_{23}$	s	$q_{i23} = \Delta u_{23}$	4'-1'	$w_{o41} = \Delta u_{41}$	s	$q_{o41} = \Delta u_{41}$

3-4	motionless	V	$q_{o34} = \Delta u_{34}$	1'-2'	motionless	V	$q_{i12} = \Delta u_{12}$
4-1	$w_{o41} = \Delta u_{41}$	s	$q_{o41} = \Delta u_{41}$	2'-3'	$w_{o23} = \Delta u_{23}$	s	$q_{i23} = \Delta u_{23}$

3.5 Cycle analysis of a VsVs discontinuous motion prototype

The cycle analysis is based on the first law. Thus, the energy transfer flows include the following energy balances derived from the previous section:

Added input heat

$$q_i = q_{i12} = u_2 - u_1 = Cv \cdot (T_2 - T_1) \tag{12}$$

Extracted output heat

$$q_o = q_{o34} = u_3 - u_4 = Cv \cdot (T_3 - T_4) \tag{13}$$

Net useful output work

$$\begin{aligned} w_o &= w_{o\exp} + |\, w_{ocont} \,| = Cv \cdot (T_2 - T_3) + Cv \cdot |\, (T_4 - T_1) \,| \\ &= (u_2 - u_3) + |\, (u_4 - u_1) \,| \end{aligned} \tag{14}$$

Therefore, the thermal efficiency is given by the ratio of the net mechanical work to the added input heat, yielding

$$\eta_{th} = \frac{w_n}{q_i} = \frac{w_{o23} + |\, w_{o41} \,|}{u_2 - u_1} = \frac{(u_2 - u_3) + |\, (u_4 - u_1) \,|}{u_2 - u_1} \tag{15}$$

However, since an important fraction of the useful work is carried out by a vacuum or thermal contraction, it is interesting to consider the proportions of useful work obtained by thermal contraction due to cooling concerning those obtained by thermal expansion.

4 Development and implementation of SSPMs-based prototypes capable of operating with TWFs obtained from Lunar ISRU components

This section focuses on developing **Self Sustaining Powered Machines (SSPMs)** [10-18] designed to operate on the surface of **Moon**. Given the planet's unique conditions, these systems must be specially engineered not only to function in the Martian environment but also to utilize locally available resources.

The most critical resources for these SSPMs are those related to **energy supply**. Thus, this section prioritizes the development of **prototypes for disruptive power supply engines**.

Table 7 outlines the potential **Thermal Working Fluids (TWFs)** present in the Lunar regolith. As such, SSPM prototypes must be capable of utilizing the gases listed in this table. The case studies presented here compare the performance of each gas as a viable TWF.

The table highlights the primary gases suitable for implementing the proposed **energy supply systems**, which consist of **cascaded Power Units (PUs)** and **Reverser Brayton Cycles (RBCs)** in cases involving self-contained heat sinks. Based on availability and suitability, **helium**, **argon and neon** emerge as the unique candidates.

Table 7: Characteristics of TWFs obtained from the Lunar ISRU regolith, useful for operating SSPMs in Martian industrial operations.

Gas names	γ=Cp/Cv	Suitability of each TWF for Lunar operations
Helium (He)	≈ 5/3	Good: Useful for SSPMs and RBCs. Highly efficient, despite providing high specific work.
Argon (Ar)	≈ 5/3	Good: Useful for SSPMs and RBCs. Highly efficient, despite providing low specific work.

Neon (Ne)	≈ 5/3	Similar to Ar, with greater soecific work than argon.

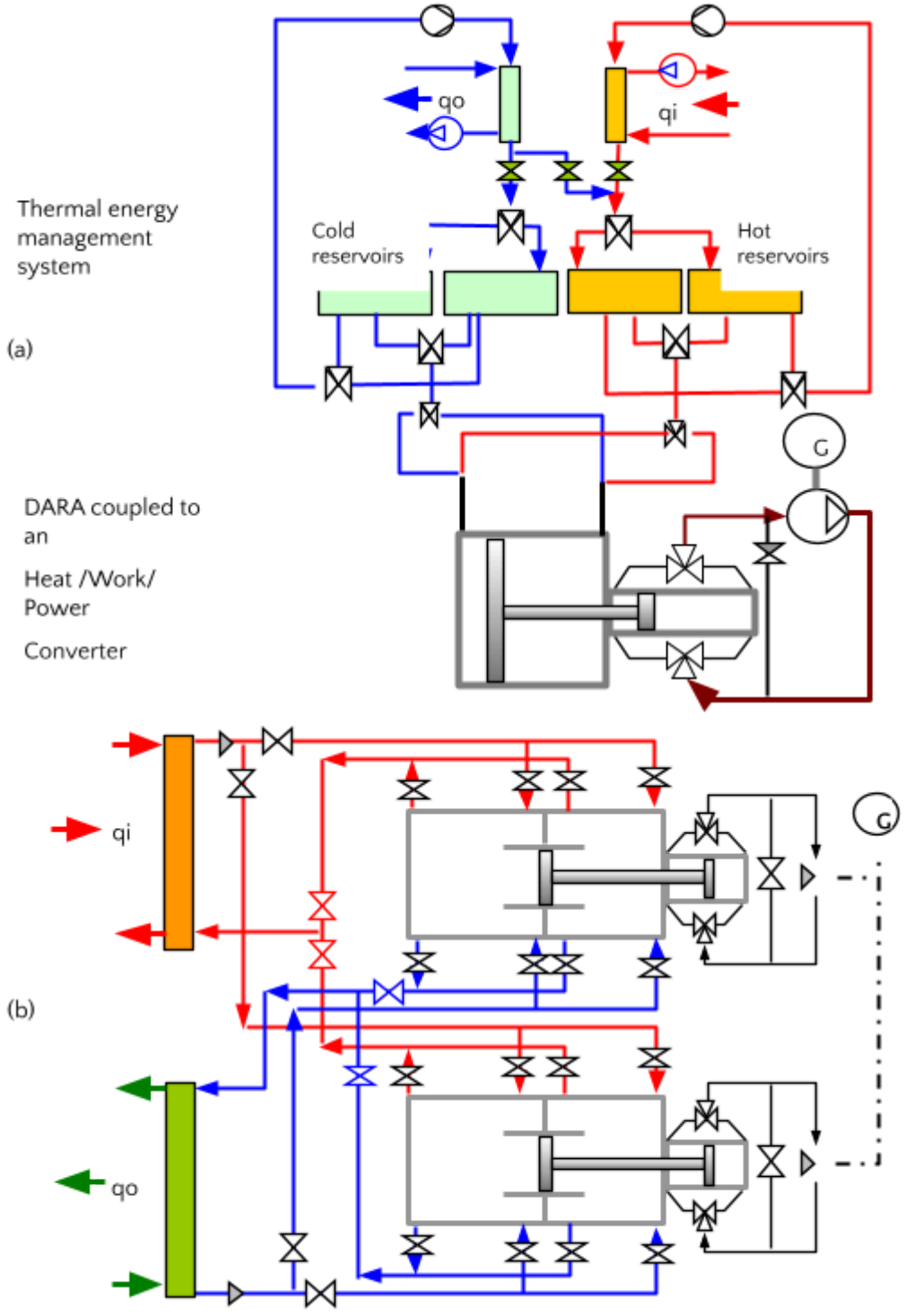

Figure 6: Illustration of the proposed double-acting reciprocating actuators (DARA): (a) illustrates the continuous motion-based DARA according to the patent P201700667. (b) Illustrates the discontinuous motion-based DARA according to the patent P202200035

The basic criteria for selecting TWFs are in situ availability, physical and chemical stability, resistance to reactions with metals, heat capacity (responsible for specific work), and adiabatic index (responsible for thermal efficiency). Table 10 therefore shows that helium is the most suitable TWF, although it has the disadvantage of a high rate of intermolecular loss, which requires regular replenishment.

To prototype PUs capable of being driven by the VsVs thermal cycle, viable physical engine structures are implemented under two core design options, both featuring the key component: the DARA. Figure 6 illustrates simplified schematics of these structures:

(a) Continuous Motion-Based DARA (Patent P201700667 [xx]): Fig. 6 (a)

This PU operates under continuous motion, meaning heat transfer occurs simultaneously with piston rod movement. As a result, this DARA model requires a feedback pump to return the TWF from the cold-side reservoirs to the warm or hot reservoirs.

(b) Discontinuous Motion-Based DARA (Patent P202200035 [YY]): Fig. 6 (b)

This PU operates under discontinuous motion, where heat transfer takes place only when the piston rod is stationary. Specifically, while one piston rod moves, its complementary rod remains motionless, and vice versa. This strategy eliminates the need for a feedback pump and external TWF reservoirs outside the actuator cylinder.

4.1 Empirical validations through case studies

Taking into account the considerations given in section 3 regarding the fulfillment of the energy conservation concepts associated with FLT, let us consider the implementation of the case study as two groups of power plant prototypes, since it is a matter of studying two Power Plant (PP) structures that fulfill two different application demands, depending on the on-site or local environment in terms of ambient heat sink temperatures:

1 Self-Sustaining Power Plant (SSPP) implemented by means of a group of cascaded of PUs characterized by its ability to operate without any external Power Supply (PS)

2 Combined-cycle structure consisting of a heat pump consisting of a Reverse Brayton Cycle (RBC) and a cascade of PUs that constitutes a SSPM. The RBC operates with Helium-4 (he-4) or Argon (Ar) or Neon (Ne) as the TWFs as illustrated by Table 11. The reason for using He, Ar and Ne as TWFs is due to the abundance of the components of ISRU on Moon surface regolith.

Fig. 6 illustrates both mentioned concepts of SSPMs [10-16]. In Fig. 6(a) it is shown a SSPM composed by a group of cascaded PUs, while in Fig 6(b) a simplified coupling scheme of a heat pump formed by the RBC with the SSPM formed by a cascade of PUs. The design of the heat pump must satisfy the condition of supplying the heat demand of the first PU of the SSPM plant, as well as absorbing the heat rejected by the last power unit of the cascaded PUs of the SSPM plant.

Fig. 6(b) illustrates a RBC coupled to a SSPM to achieve the self-heat source (SHS) and a self-heat sink (SHSk) giving rise to a complete autonomous SSPM enabled to operate without any external power source and power sink, which defy some second law statements. In the concerned case study a reversed Brayton cycle (RBC) is combined with a cascade of PUs enabled to perform useful mechanical work under operational self-sufficiency. The function of the RBC is to perform the functions of a thermal energy supply source and a thermal energy sink source while the cascade of PUs is responsible for transforming the thermal energy into work and/or electrical power.

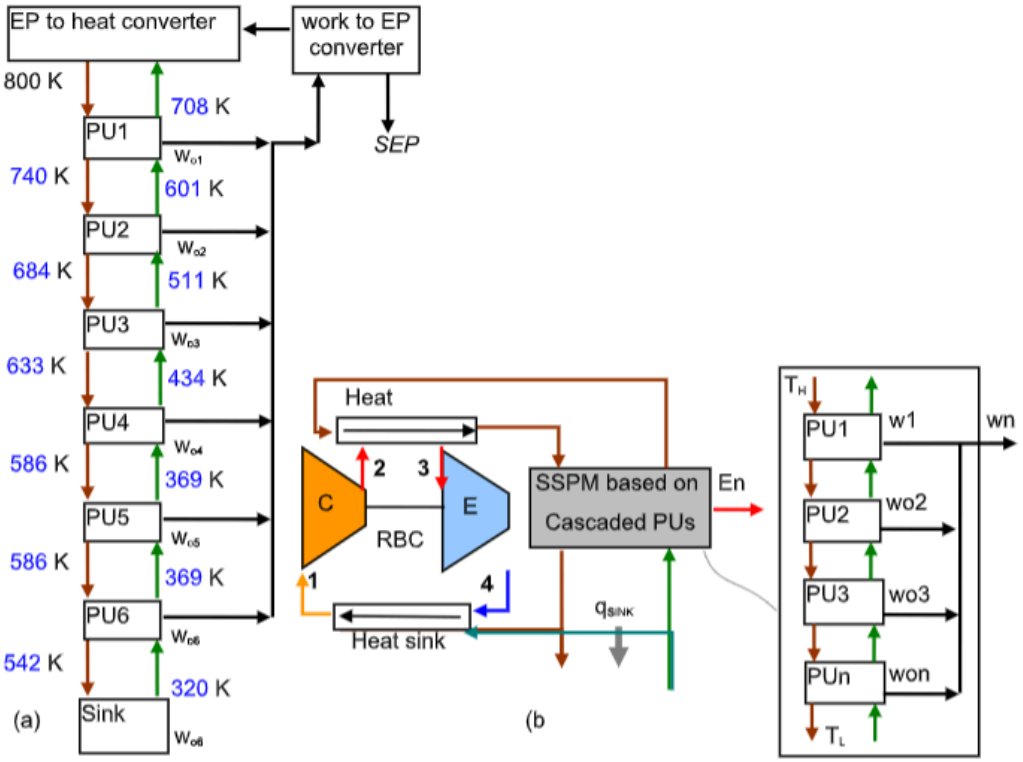

Figure 7: Schematic structure a CC composed by a SSPM coupled to the RBC [19-21]. (a) Depicts the HP based on a RBC. (b), illustrates the SSPM composed by a cascade of 6 PUs

4.2 Implementing Case Studies Aimed at Prototyping SSPMs and CCs Based on (RBC-SSPM)

The study of the different cycles concerns the local resources of thermal working fluids that either exist in the Martian atmosphere or can be obtained from it. Therefore, Table 8 illustrates the possible combinations of plant structures based on SPMs and TWFs compatible with such plant structures. According to the table data, He, Ar and Ne are applied to the RBS for the three case studies-based plant structure combinations, while the SSPMs based on Cascaded PUs can operate with the same TWFs.

Table 8: Available TWFs and compatibility to be used on SSPMs based on both a group of cascaded PUs and a CC-based (RBC-SSPM)

Available TWFs	TWF for SSPMs	TWFs for CCs based on (RBC-SSPMs)
He-4	He-4	He-He
Ar	Ar	Ar- Ar
Ne	Ne	Ne- Ne

In summary, both PPs composed of a group of cascaded PUs (SSPMs) and PPs composed of a combined cycle (CC) composed of the combination of an SSPM and a reverse Brayton cycle (RBS) are designed to operate with the same TWF in each case.

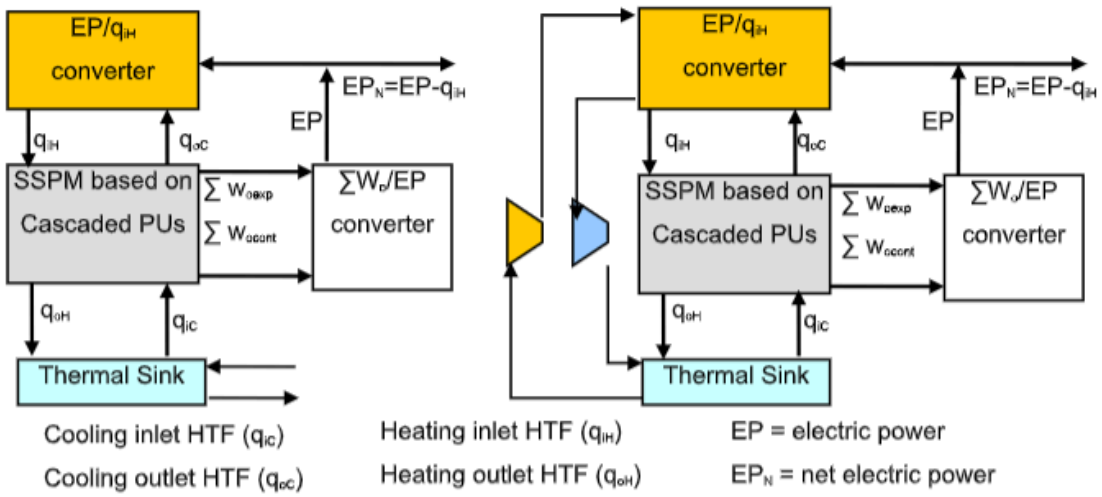

Figure 8: Block diagrams of the energy flows. (a) Illustrates a general scheme of SSPM with external heat sink. (b) Illustrates a general scheme of CC based (RBC-SSPM)without external heat sink.

Fig. 8 illustrates the general schemes corresponding to the SSPM depicted in Fig. 8 (a) and the CC based on the combination of a RBC and a SSPM composed of a set of cascaded PUs depicted in Fig. 4 (b) similar to that of Fig. 8(a). If we consider the practical application site as Moon, the combined cycle option shown in Fig. 8(b) is not necessary since there is a natural heat sink in the Martian atmosphere due to its low mean temperature. Therefore, a SSPM is sufficient, simpler, less expensive, and easier to maintain.

4.3 Heat Pump as heat source and sink with helium as TWF

The thermodynamic study of the heat pump based on a RBC is carried out using the data from [15] for Helium as real TWF. Therefore, Table 9 depicts the data corresponding to the open-process-based RBC responsible for performing the tasks of heat supply power source and heat sink, both operating as a heat pump with argon as the TWF. The general structure of the heat pump-based RBS is represented in Fig 7(b).

The heat pump is implemented by means of a RBC responsible for supplying heat to the associated group of cascaded PUs and extract heat from the group of cascaded PUs that give rise t a SSPM. Thus, the sequence of open processes corresponds to the RBC structure depicted in Fig. 7(b). Used data has been taken from the database from NIST. The design criteria for both heat and cold sources are more in line with the need to satisfy the cold and heat demands to feed the PU cascade than to obtain a high COP value.

Table 13 illustrates the main RBC results operating as heat pump with He as TWF. The results derived from the heat pump implemented by means of a RBC operating under open system-based processes and computed with data from Table 9. Inlet compressor pressure p_1=10 bar; outlet compressor pressure p_2=15.5; compressor pressure ratio (PR)=1.55. Since the RBC is responsible for supplying the demanded amount of heat as well as the demanded amount of cold to ensure the isolated heat sink tasks, let's consider the relevance of the data shown in Table 13. Therefore, in order to supply the necessary heat and dissipate the rejected heat to/from the SSPM consisting of a group of cascaded PUs, an energy balance of heat input and dissipation is carried out using a heat dissipation energy balance to obtain the flow rate of heat dissipation fluid through the RBC. This determines the RBC cycle stress so that it meets the heat sink demand. This results in excess high-grade thermal energy produced by the RBC compressor, which can be utilized both as direct heat and to power other devices, including another power plant. The methodology used to resolve the case studies have been described an applied in a previous work referenced as [18].

The CC operating with Helium as TWF composed by a HP based on a RBS and a SSPM consisting of a group of 6 cascaded PUs operating by the VsVs cycle, is depicted in Tables 9, 10, 11, 12 and 13.

Table 9: Illustration of the RBC data corresponding to He as TWF enabled to operate as heat pump to provide a SHS for self-input heat and a SHSk to absorb the heat released by the SSPM.

RB-He-4	T(K)	p(bHe)	V(m^3/kg)	u(kJ/kg)	h(kJ/kg)	h'(kJ/kg)	s(kJ/kg-K)
1	680.00	10	1.4151	2124.40	3539.5	3539.5	27.475
2	810.00	15.486	1.0890	2529.80	4291.4	4216.2	27.475
2a	690.00	15.486	0.9281	2155.80	3593.1	3593.1	26.642

3	340.00	15.486	0.4590	1065.00	1775.8	1775.8	22.967
4	285.43	10	0.5959	894.74	1519.1	1490.6	22.967
4a	340.00	10	0.7092	1064.80	1774	1774	28.658

The RBC computed with the data from Table 12 is depicted in Table 10. The relevant data depicted in this table deals with the parameters that sustain the heat source and heat sink, that are: Available Self Heat Source (SHS) (kJ/kg) = **698.3** and Available Self Heat Sink (SHSk) (kJ/kg) = **254.9**, while the amount of work demanded by the heat pump, which must be extracted from the SSPM, approaches **-495.2** (kJ/kg).

Table 10: Depiction of the RBC results operating with **He-4** as TWF

Work done on the compressor of the RBC (kJ/kg)	W_{i12}= w_{i_comp} (kJ/kg)	752.00
Total pumped heat (kJ/kg)	q_{o23} (kJ/kg)	2515.60
Work done on by the expander of the RBC (kJ/kg)	W_{o34} = w_{o_exp} (kJ/kg)	256.70
Total recovered heat to the compressor suction side (kJ/kg)	q_{i41} (kJ/kg)	2020.40
Isentropic efficiency	Is_eff (%)	90
w_n (RBC)=w_{i_comp}-w_{o_exp}=q_i-q_o(kJ/kg)	RBC work demand (kJ/kg)	**-495.21**
Coefficient of performance for the RBC	COP	5.71
Available Self Heat Source (SHS) (kJ/kg)	Available SHS_(q_{o2-2a}) RBC (kJ/kg)	**698.3**
Available Self Heat Sink (SHSk) (kJ/kg)	Available SHSk_(q_{i4-4a}) RBC (kJ/kg)	**254.9**

Table 11 shows the heat flow ratios corresponding to SHSk and SHS formed by the RBC to extract and add the required heat from/to the cascade PU group. If the group of cascaded PUs that conform the SSPM operates with He-4 as TWF, then the second column of Table 11 shows the CCF corresponding to He-4.

Table 11: Illustration of the Cooling Capacity and Heating Capacity factors using He-4 for both, the RBC-based heat pump and the group of cascade PUs.

Cooling Capacity factor (CCF) (kJ/kg RBC)/(kJ/kg PU6)	**1.63**
heating capacity factor (HCF) (kJ/kg) RBC/ (kJ/kg PU1)	**1.87**

4.3.1 Studying the SSPMs operated by the cycle VsVs with helium as TWF for all PUs

The cascaded PUs operating with a VsVs cycle responsible for converting the heat and cold obtained from the heat pump implemented by the RBC as available SHS and available SHSk is depicted in Table 12. The ratio of cascaded temperatures (RIT) is selected as 0.85 for all TWF and the losses inherent to irreversibilities LS (%) and RF (%) are assumed as 0.85 and 0,95 respectively. Table 12 shows set of six cascaded PUs operating with **He** as TWF on the set of six cascaded VsVs cycles.

Table 12: Illustration of the set of 6 PUs operating in cascade; table data corresponds to the real gas He as TWF. Table values are taken from reference [NIST] for all considered gases

PU1-He	**T(K)**	**p(bar)**	**v(m^3/kg)**	**u(kJ/kg)**	**s(kJ/kg.K)**
1	680.00	10	1.41510	2124.40	27.475
2	800.00	11.7640	1.41510	2498.40	27.981
3	749.64	10	1.55980	2341.40	27.981
4	637	0.8497	1.55980	1989.90	27.475
PU2-He	**T(K)**	**p(bar)**	**v(m^3/kg)**	**u(kJ/kg)**	**s(kJ/kg.K)**
1	578.00	10	1.20330	1806.50	26.631
2	680.00	11.7640	1.20330	2124.50	27.137
3	637.14	10	1.32620	1991.00	27.137
4	542.00	8.5069	1.32620	1694.30	26.631
PU3-He	**T(K)**	**p(bar)**	**v(m^3/kg)**	**u(kJ/kg)**	**s(kJ/kg.K)**

1	491.30	10	1.0233	1536.40	25.787
2	578.00	11.7640	1.0233	1806.60	26.293
3	541.59	10	1.1277	1692.60	26.293
4	460.60	8.5054	1.1277	1440.60	25.787
PU4-He	**T(K)**	**p(bar)**	**v(m^3/kg)**	**u(kJ/kg)**	**s(kJ/kg.K)**
1	417.61	10	0.87032	1306.70	24.943
	491.30	11.7640	0.87032	1536.60	25.450
3	460.44	10	0.95923	1440.20	25.450
4	391.50	8.5035	0.95923	1225.30	24.943
PU5-He	**T(K)**	**p(bar)**	**v(m^3/kg)**	**u(kJ/kg)**	**s(kJ/kg.K)**
1	354.96	10	0.74024	1111.40	24.152
	417.61	11.7640	0.74024	1306.80	24.606
3	391.36	10	0.81582	1224.90	24.606
4	332.70	8.50170	0.81582	1042.00	24.152
PU6-He	**T(K)**	**p(bar)**	**v(m^3/kg)**	**u(kJ/kg)**	**s(kJ/kg.K)**
1	301.72	10	0.62970	945.49	23.255
	354.96	11.7640	0.62970	1111.50	23.762
3	332.65	10	0.69394	1041.90	23.762
4	282.60	8.49580	0.69394	885.84	23.255

Table 13 illustrates the results corresponding to a group of six cascaded PUs operated by a VsVs cycle with He as real TWF.

Table 13: Illustration of the results set of 6 PUs operating in cascade with real gas He as TWF depicted in Table 15

PUi-Her	1	2	3	4	5	6	total
LF(%)	0.85	0.85	0.85	0.85	0.85	0.85	0.85
RF(%)	0.95	0.95	0.95	0.95	0.95	0.95	0.95
RIT*100	85.0	85.0	85.0	85.0	85.00	85.0	85.00
T2(K)	800.00	680.00	578.00	491.30	417.61	354.96	
T1(K)	680.00	578.00	491.30	417.61	354.96	301.72	
qi_12/PU(kJ/kg)	374.00	318.00	270.20	229.90	195.40	166.01	1553.51
qo_34(kJ/kg)	351.50	296.70	252.00	214.90	182.90	156.06	1454.06
q_recov(kJ/kg)	333.93	281.87	239.40	204.16	173.76	148.26	1381.36
Tm_qrecov(kJ/kg)	693.32	589.57	501.10	425.97	362.03	307.63	
wn(kJ/kg)	235.39	198.40	169.41	143.57	122.17	104.37	**973.32**
η_th/PU(%)	53.50	53.03	53.29	53.08	53.15	53.44	
η_th/plant(%)							260.25
SSI(%)							**160.25**
wnn(kJ/kg)/cycle	Total net work out = wn(SSPM)*CCF(SHSk) - wn(RBC)=						**1094.435**

4.4 Heat Pump as heat source and sink with argon as TWF

The thermodynamic study of the heat pump based on a RBC is carried out using the data from NIST for Argon as real TWF. Therefore, Table 17 depicts the data corresponding to the open-process-based RBC responsible for performing the tasks of heat supply power source and heat sink, both operating as a heat pump with Argon as the TWF. The general structure of the heat pump-based RBS is represented in Fig 7(b). The CC operating with

Argon as TWF composed by a HP based on a RBS and a SSPM consisting of a group of 6 cascaded PUs operating by the VsVs cycle, is depicted in Tables 14, 15, 17 and 18.

The same computation structure and results has bee3n adopted from the argon as TWF. The methodology used to resolve the case studies have been described an applied in a previous work referenced as [18].

Table 14: Illustration of the RBC data corresponding to Ar as TWF enabled to operate as heat pump to provide a SHS for self-input heat and a SHSk to absorb the heat rejected by the SSPM.

RB-Ar	T(K)	p(bar)	V(m^3/kg)	u(kJ/kg)	h(kJ/kg)	h'(kJ/kg)	s(kJ/kg-K)
1	680.00	1	1.4157	212.24	353.8	353.8	4.3051
2	810.00	1.5489	1.0889	252.81	429.0	421.5	4.3051
2a	690.00	1.5489	0.9276	215.33	359	359	4.2216
3	340.00	1.5489	0.4567	105.94	176.7	176.7	3.8529
4	286.00	1	0.5917	89.12	148.6	148.6	3.8529
4a	340.00	1	0.7075	106.01	176.75	176.75	3.9442

The RBC computed with the data from Table 14 is depicted in Table 15.

Table 15: Depiction of the RBC results operating with Ar as TWF

Work done on the compressor of the RBC (kJ/kg)	W_{i12}= w_{i_comp} (kJ/kg)	75.19
Total pumped heat (kJ/kg)	q_{o23} (kJ/kg)	253.33
Work done on by the expander of the RBC (kJ/kg)	W_{o34} = w_{o_exp} (kJ/kg)	28.7
Total recovered heat to the compressor suction side (kJ/kg)	q_{i41} (kJ/kg)	14.79
Isentropic efficiency	Is_eff (%)	90
w_n (RBC)=w_{icomp}-w_{oexp}=q_i-q_o(kJ/kg)	RBC work demand (kJ/kg)	**-47.12**
Coefficient of performance for the RBC	COP	5.71
Available Self Heat Source (SHS) (kJ/kg)	Available SHS_(q_{o2-2a}) RBC (kJ/kg)	**70.0**
Available Self Heat Sink (SHSk) (kJ/kg)	Available SHSk_(q_{i4-4a}) RBC (kJ/kg)	**28.2**

Table 16 shows the heat flow ratios corresponding to SHSk and SHS formed by the RBC to extract and add the required heat from/to the cascade PU group. If the group of cascaded PUs that conforms the SSPM operates with Ar as TWF, then the second column of Table 19 shows the CCF and the HCF ration corresponding to Ar

Table 16: Illustration of the Cooling Capacity and Heating Capacity factors using Ar for both, the RBC-based heat pump and the group of cascade PUs

Cooling Capacity factor (CCF) (kJ/kg RBC)/(kJ/kg PU6) =	**1,81**
heating capacity factor (HCF) (kJ/kg) RBC/(kJ/kg PU1) =	**1,87**

4.4.1 Studying the SSPMs operated by the cycle VsVs with Argon in each group of six cascaded PUs

Table 17 depicts a set of six cascaded PUs operating with **Ar** as TWF on the VsVs cycle is depicted.

Table 17: Illustration of the set of 6 PUs operating in cascade; table data corresponds to the real gas Argon as TWF. Values are taken from reference [NIST] for all considered gases

PU1-Ar	**T(K)**	**p(bar)**	**v(m^3/kg)**	**u(kJ/kg)**	**s(kJ/kg.K)**
1	680.00	10.000	0.14190	211.79	3.825
2	800.00	11.770	0.14190	249.29	3.876
3	750.00	10.000	0.15623	233.71	3.876
4	635.00	8.478	0.15623	197.78	3.825
PU2-Ar	**T(K)**	**p(bar)**	**v(m^3/kg)**	**u(kJ/kg)**	**s(kJ/kg.K)**
1	578.00	10	0.12058	179.82	3.740

2	680.00	11.7730	0.12058	211.71	3.791
3	637.00	10	0.13283	198.32	3.791
4	541.00	8.4920	0.13283	168.32	3.740
PU3-Ar	**T(K)**	**p(bar)**	**v(m^3/kg)**	**u(kJ/kg)**	**s(kJ/kg.K)**
1	491.30	10	0.10242	152.60	3.655
2	578.00	11.7770	0.10242	179.71	3.706
3	543.00	10	0.11236	168.84	3.706
4	462.00	8.5669	0.11236	143.51	3.655
PU4-Ar	**T(K)**	**p(bar)**	**v(m^3/kg)**	**u(kJ/kg)**	**s(kJ/kg.K)**
1	417.61	10	0.08695	129.41	3.570
	491.30	11.7830	0.08695	152.46	3.621
3	461.00	10	0.09566	143.07	3.621
4	398.70	8.6731	0.09566	123.58	3.570
PU5-Ar	**T(K)**	**p(bar)**	**v(m^3/kg)**	**u(kJ/kg)**	**s(kJ/kg.K)**
1	354.96	10	0.07373	109.61	3.484
	417.61	11.7930	0.07373	129.23	3.535
3	392.00	10	0.08098	121.32	3.535
4	333.00	8.5348	0.08098	102.84	3.484
PU6-Ar	**T(K)**	**p(bar)**	**v(m^3/kg)**	**u(kJ/kg)**	**s(kJ/kg.K)**
1	301.72	10	0.06244	92.69	3.398
	354.96	11.8050	0.06244	109.39	3.449
3	332.10	10	0.06885	102.36	3.449
4	282.50	8.4824	0.06885	86.79	3.398

Table 18 illustrates the results corresponding to a group of six cascaded PUs operated by a VsVs cycle with Argon as real TWF.

Table 18: Illustration of the results set of 6 PUs operating in cascade with real gas Argon as TWF depicted in Table 17 -20

PU-Ar	1	2	3	4	5	6	total
LF(%)	0.85	0.85	0.85	0.85	0.85	0.85	0.85
RF(%)	0.95	0.95	0.95	0.95	0.95	0.95	0.95
RIT*100	85.0	85.0	85.0	85.0	85.00	85.0	85.00
T2(K)	800.00	680.00	578.00	491.30	417.61	354.96	
T1(K)	680.00	578.00	491.30	417.61	354.96	301.72	
qi_12/PU(kJ/kg)	37.50	31.89	27.11	23.05	19.62	16.70	155.87
qo_34(kJ/kg)	35.93	30.00	25.33	19.49	18.48	15.57	144.80
q_recov(kJ/kg)	34.13	28.50	24.06	18.52	17.56	14.79	137.56
Tm_qrecov(kJ/kg)		589.00	502.50	429.85	362.50	307.30	
wn(kJ/kg)	23.89	20.10	16.12	12.29	11.85	10.44	**94.69**
η_th/PU(%)	63.72	63.03	59.45	53.32	60.42	62.48	
η_th/plant(%)							252.51
SSI(%)							**152.51**

wnn(kJ/kg)/cycle	**Total net work out = wn(SSPM)*CCF(SHSk) - wn(RBC)=**	**124.111**

4.5 Heat Pump as heat source and sink with Neon as TWF

The thermodynamic study of the heat pump based on a RBC is carried out using the data from [15] for Neon as real TWF. Therefore, Table 12 depicts the data corresponding to the open-process-based RBC responsible for performing the tasks of heat supply power source and heat sink, both operating as a heat pump with Neon as the TWF. The general structure of the heat pump-based RBS is represented in Fig 7(b). The CC operating with Neon as TWF composed by a HP based on a RBS and a SSPM consisting of a group of 6 cascaded PUs operating by the VsVs cycle, is depicted in Tables 19, 20, 21, 22 and 23.

Table 19: Illustration of the RBC data corresponding to Neon as TWF enabled to operate as heat pump to provide a SHS for self input heat and a SHSk to absorb the heat rejected by the SSPM.

RBC-Ne	T(K)	p(bar)	V(m^3/kg)	u(kJ/kg)	h(kJ/kg)	h'(kJ/kg)	s(kJ/kg-K)
1	593.30	10	0.24513	426.31	671.4	671.4	5.4448
2	698.00	15.015	0.1922	491.08	791.7	779.7	5.4448
2a	590.00	15.015	0.16257	424.27	668.37	668.37	5.2716
3	285.00	15.015	0.0788	235.33	353.6	353.6	4.5205
4	242.30	10	0.1003	208.98	309.3	309.3	4.5205
4a	280.00	10	0.1159	232.37	348.31	348.31	4.6702

Table 20: Depiction of the RBC results operating with **Ne** as TWF

Work done on the compressor of the RBC (kJ/kg)	W_{i12}= w_{i_comp} (kJ/kg)	120.26
Total pumped heat (kJ/kg)	q_{o23} (kJ/kg)	438.09
Work done on by the expander of the RBC (kJ/kg)	W_{o34} = w_{o_exp} (kJ/kg)	44.28
Total recovered heat to the compressor suction side (kJ/kg)	q_{i41} (kJ/kg)	362.11
Isentropic efficiency	Is_eff (%)	90
w_n (RBC)=w_{i_comp}-w_{o_exp}=q_i-q_o(kJ/kg)	RBC work demand (kJ/kg)	-76.00
Coefficient of performance for the RBC	COP	5.71
Available Self Heat Source (SHS) (kJ/kg)	Available SHS_(q_{o2-2a}) RBC(kJ/kg)	**698.3**
Available Self Heat Sink (SHSk) (kJ/kg)	Available SHSk_(q_{i4-4a}) RBC(kJ/kg)	**254.9**

Table 21 shows the heat flow ratios corresponding to SHSk and SHS formed by the RBC to extract and add the required heat from/to the cascade PU group. If the group of cascaded PUs that conform the SSPM operates with Neon as TWF, then the second column of Table 21 shows the CCF corresponding to Neon.

Table 21: Illustration of the Cooling Capacity and Heating Capacity factors using Neon for both, the RBC-based heat pump and the group of cascade PUs

Cooling Capacity factor (CCF) (kJ/kg RBC)/(kJ/kg PU6):	**1.46**
heating capacity factor (HCF) (kJ/kg)RBC/(kJ/kg-PU1) = (SHS_qo2-2a_RBC)/(qi12-PU1)=698.2/95.7:	**1.90**

4.5.1 Studying the SSPMs operated by the cycle VsVs with Neon in each group of six cascaded PUs

In Table 22 it is depicted the set of 6 PUs operating in cascade; table data corresponds to the real gas Neon as TWF. Values are taken from reference [NIST] for all considered gases

Table 22: Illustration of the set of 6 PUs operating in cascade; table data corresponds to the real gas Argon as TWF. Values are taken from reference [NIST] for all considered gases

PU1- Ne	**T(K)**	**p(bar)**	**v(m^3/kg)**	**u(kJ/kg)**	**s(kJ/kg.K)**
1	593.30	10.000	0.24513	426.31	5.445

2	698.00	11.764	0.24513	491.07	5.545
3	654.00	10.000	0.27002	463.85	5.545
4	557.00	8.521	0.27002	403.86	5.445
PU2- Ne	**T(K)**	**p(bar)**	**v(m^3/kg)**	**u(kJ/kg)**	**s(kJ/kg.K)**
1	504.31	10	0.20845	371.27	5.277
2	593.30	11.7650	0.20845	426.31	5.378
3	556.05	10	0.22979	403.27	5.378
4	472.00	8.4877	0.22979	351.29	5.277
PU3- Ne	**T(K)**	**p(bar)**	**v(m^3/kg)**	**u(kJ/kg)**	**s(kJ/kg.K)**
1	428.66	10	0.17727	324.46	5.110
2	504.31	11.7660	0.17727	371.26	5.210
3	472.50	10	0.19527	351.59	5.210
4	402.00	8.5105	0.19527	307.97	5.110
PU4- Ne	**T(K)**	**p(bar)**	**v(m^3/kg)**	**u(kJ/kg)**	**s(kJ/kg.K)**
1	364.36	10	0.15076	284.65	4.942
	428.66	11.7660	0.15076	324.44	5.043
3	401.80	10	0.16619	307.83	5.043
4	341.30	8.4933	0.16619	270.40	4.942
PU5- Ne	**T(K)**	**p(bar)**	**v(m^3/kg)**	**u(kJ/kg)**	**s(kJ/kg.K)**
1	309.71	10	0.12820	250.79	4.774
	364.36	11.7680	0.12820	284.62	4.875
3	341.40	10	0.14130	270.43	4.875
4	290.00	8.4911	0.14130	238.62	4.774
PU6- Ne	**T(K)**	**p(bar)**	**v(m^3/kg)**	**u(kJ/kg)**	**s(kJ/kg.K)**
1	263.25	10	0.10901	221.98	4.607
	309.71	11.7700	0.10901	250.75	4.707
3	290.14	10	0.12013	238.66	4.707
4	247.00	8.5089	0.12013	211.96	4.607

Table 23 illustrates the results corresponding to a group of six cascaded PUs operated by a VsVs cycle with Argon as real TWF.

Table 23: Illustration of the results set of 6 PUs operating in cascade with real gas Neon as TWF depicted in Table 22

PUi-Her	1	2	3	4	5	6	total
LF(%)	0.85	0.85	0.85	0.85	0.85	0.85	0.85
RF(%)	0.95	0.95	0.95	0.95	0.95	0.95	0.95
RIT*100	85.0	85.0	85.0	85.0	85.00	85.0	85.00
T2(K)	698.00	593.30	504.31	428.66	364.36	309.71	
T1(K)	593.30	504.31	428.66	364.36	309.71	263.25	
qi_12/PU(kJ/kg)	64.76	55.04	46.80	39.79	33.83	28.77	268.99
qo_34(kJ/kg)	59.99	51.98	43.62	37.43	31.81	26.70	251.53
q_recov(kJ/kg)	56.99	49.38	41.44	35.56	30.22	25.37	238.95

Tm_qrecov(kJ/kg)		514.03	437.25	371.55	315.70	268.57	
wn(kJ/kg)	40.11	34.74	29.20	24.92	21.29	17.85	**168.11**
η_th/PU(%)	61.93	63.12	62.39	62.63	62.92	62.06	
η_th/plant(%)							259.58
SSI(%)							**159.58**
wnn(kJ/kg)/cycle	**Total net work out = wn(SSPM)*CCF(SHSk) - wn(RBC)=**						**169.45**

5 Analysis of results

A summary of the three case studies concerning to the viable CCs on the Moo surface operating with Helium, Argon, and Neon as available in-situ TWFs are considered and depicted in Table 24.

Table 24: Summary of results from Tables 13, 18 and 23 for He, Ar, and Ne respectively

PU-He	1	2	3	4	5	6	total
wn(kJ/kg)	41.03	34.70	29.31	24.82	21.54	17.82	973.32
η_th/plant(%)							260.25
SSI (%)							160.25
wnn(kJ/kg)/cycle	**Total net work out = wn(SSPM)*CCF(SHSk) - wn(RBC)=**						1094.435
PU-Ar	1	2	3	4	5	6	total
wn(kJ/kg)	23.89	20.10	16.12	12.29	11.85	10.44	94.69
η_th/plant(%)							252.51
SSI (%)							152.51
wnn(kJ/kg)/cycle	**Total net work out = wn(SSPM)*CCF(SHSk) - wn(RBC)=**						124.111
PU-Ne	1	2	3	4	5	6	total
wn(kJ/kg)	40.11	34.74	29.20	24.92	21.29	17.85	168.11
η_th/plant(%)							269.45
SSI(%)							169.45
wnn(kJ/kg)/cycle	**Total net work out = wn(SSPM)*CCF(SHSk) - wn(RBC)=**						169.45

Table 25 illustrates the most relevant results concerning to SSPMs and CC-based (RBS-SSPMs) operating with ISRU-based Helium, Argon and Neon as TWFs.

Table 25: Summary of main results for SSPMs and CC-based (RBS-SSPM)

	He	**Ar**	**Ne**
Net SSPM work (kJ/kg)	973.32	94.70	168.11
Self-Sufficient Index [SSI (%)]	160.25	152.50	159.58
Net CC-based (RBS-SSPM) work (kJ/kg)/cycle	1094.435	124.10	169.45

With reference to the results illustrated in Tables 24 and 25 a concise analysis of the most relevant results is presented, highlighting key findings and performance analysis

5.1 Summary of findings and Discussion

The study presents a comprehensive analysis of **Self-Sustaining Power Machines (SSPMs)** designed for lunar operations, focusing on **in-situ resource utilization (ISRU)** and the thermodynamic behavior of **thermal working fluids (TWFs)**—helium (He), argon (Ar), and neon (Ne). The results highlight the feasibility of SSPMs in lunar environments, their energy efficiency, and the challenges associated with their implementation.

5.1.1 Key Findings:

Lunar Resource Viability

Helium-3 (^{3}He), argon, and neon are identified as critical resources for SSPMs due to their presence in lunar regolith and suitability as TWFs.

Water ice (~1.6B metric tons in Polar Regions) is a high-priority resource for life support and fuel production.

Exosphere gases (He, Ar, Ne) are impractical for direct extraction but can be obtained from regolith processing.

5.1.2 Thermodynamic Performance of SSPMs

Helium exhibits the highest **net work output (973.32 kJ/kg)** and **Self-Sufficient Index (SSI = 160.25%)**, making it the most efficient TWF.

Argon has the lowest performance (**94.70 kJ/kg net work, SSI = 152.50%**) but remains viable due to its abundance.

Neon shows intermediate performance (**168.11 kJ/kg net work, SSI = 159.58%**), balancing efficiency and availability.

5.1.3 Combined Cycle (RBC-SSPM) Performance

The **RBC-based heat pump** enhances SSPM efficiency by providing **self-sustaining heat sources (SHS) and sinks (SHSk)**. Having the ability to generate energy without the need for an external power source or sink allows us to operate in environments with temperatures that can range from almost zero Kelvin to over 1200 K, taking into account that in high temperature environments it is possible to cool the envelopes of the interior environments of any habitat with the energy generated itself.

Helium-based CC achieves the highest **net work output (1094.43 kJ/kg/cycle)**.

Argon and neon-based CCs show lower but still viable outputs (**124.10 kJ/kg and 169.45 kJ/kg, respectively**).

5.1.4 Thermal Efficiency and Energy Balance

The **VsVs thermal cycle** (used in SSPMs) demonstrates **unprecedented efficiencies (>250%)**, challenging conventional thermodynamic limits.

Contraction-based work extraction (pull forces) contributes to increased internal energy, contradicting the First Law of Thermodynamics (FLT) but validated experimentally.

5.2 Discussion

5.2.1 Implications for Lunar Industrialization

SSPMs enable fully autonomous power generation without reliance on solar or nuclear fusion, crucial for long-term lunar habitation.

Helium-3 mining (despite high energy demands) remains a strategic goal due to its applications in **fusion energy, cryogenics, and medical imaging**.

Water and metal extraction (Si, Al, Fe) are essential for **construction and life support**, but require energy-intensive processing.

5.2.2 Challenges and Limitations

Energy-intensive extraction: Processing **150 tons of regolith for 1g of ^{3}He** demands massive power infrastructure.

Thermodynamic anomalies: The **contradiction between FLT and experimental observations** (suction/contraction work) requires further theoretical refinement.

Material durability: TWFs like helium have **high intermolecular loss rates**, necessitating replenishment.

5.2.3 Future Prospects

Advanced ISRU technologies: Improved **regolith processing and gas extraction** could reduce energy costs.

Hybrid power systems: Combining **SPMs with solar/nuclear** could enhance reliability.

Legal and commercial frameworks: The **Artemis Accords** must address **lunar mining rights** to avoid conflicts.

6. General Conclusions

This study presents a pioneering framework for the design and implementation of **Self-Sustaining Power Machines (SSPMs)** on the Moon, leveraging **in-situ resource utilization (ISRU)** to enable autonomous energy generation. By challenging conventional thermodynamic principles and introducing innovative hybrid systems, the work advances the feasibility of sustainable lunar operations. The key conclusions are as follows:

Key Contributions

Breakthrough in Thermodynamics: The proposed **Hybrid Isolated System (HIS)**, integrating a Reverse Brayton Cycle (RBC) heat pump with cascaded SSPM units, operates **without external heat sources or sinks**, defying traditional interpretations of the First and Second Laws of Thermodynamics (FLT/SLT).

The **VsVs thermal cycle** achieves unprecedented efficiencies (>250%), enabled by contraction-based work extraction (pull forces), which experimentally demonstrates energy gains contradicting classical FLT assumptions.

Performance of Lunar-Derived Working Fluids: **Helium (He)** emerges as the highest-performing thermal working fluid (TWF), delivering a net work output of **973.32 kJ/kg** and a Self-Sufficient Index (SSI) of **160.25%**.

Argon (Ar) and **Neon (Ne)**, while less efficient, remain viable due to lunar abundance, with Argon showing promise in combined-cycle (RBC-SSPM) configurations.

CO_2 is deemed impractical for high-efficiency power generation despite its lunar availability.

Feasibility of ISRU-Based Energy Systems: SSPMs offer a **maintenance-free, fuel-independent** alternative to nuclear or solar power, critical for long-term lunar habitation and industrial operations.

The combined cycle (RBC-SSPM) demonstrates **self-sustaining net work output**, with helium-based systems achieving**1094.43 kJ/kg/cycle**.

Theoretical and Practical Implications

Reinterpretation of Thermodynamics: The findings necessitate revisiting FLT/SLT to account for **pull-force work** and hybrid isolated systems, potentially reshaping energy conversion theories.

Energy Independence: SSPMs enable **fully autonomous power generation** in extreme environments (e.g., lunar shadows, deep space), reducing reliance on Earth-supplied resources.

Lunar Industrialization: The study supports **helium-3 mining** and water extraction as strategic priorities, though challenges like regolith processing energy costs persist.

Limitations and Future Work: While empirically validated through case studies, the results depend on prior theoretical frameworks ([12–19]). To solidify these advancements, the following are critical:

Experimental Prototyping: Rigorous testing of SSPM units under lunar-simulated conditions to validate efficiency claims and thermodynamic anomalies.

ISRU Optimization: Development of low-energy regolith processing methods for TWF extraction (e.g., helium-3 separation).

Hybrid System Integration: Coupling SSPMs with solar/nuclear systems for redundancy and scalability.

Policy Development: Alignment with the **Artemis Accords** to address lunar mining rights and resource governance.

Final Recommendations:

--Prioritize **helium-based SSPMs** for high-demand applications, with argon/neon as backups.

--Invest in **material science** to mitigate TWF leakage (e.g., helium's intermolecular losses).

--Foster interdisciplinary collaboration to refine thermodynamic models and accelerate prototype deployment.

This research marks a **paradigm shift** in extraterrestrial energy systems, laying the groundwork for **self-sufficient lunar colonies** and deep-space exploration. By bridging theoretical innovation with practical ISRU strategies, SSPMs could revolutionize humanity's approach to sustainable off-world power.

References

1 Yulia Akisheva, et. al. Regolith-based Lunar Habitats - an Engineering Approach to Radiation Shielding. Aerospace Europe Conference– 10TH EUCASS – 9TH CEAS. 2023. DOI: 10.13009/EUCASS2023-879. https://www.bing.com/search?q=Sustainable+Energy+Architectures+for+Lunar+Habitats&form=ANNH01&refig=5558df4248b24e16b70dce4d0bd03747&pc=EDGEESS. Retrieved from:

2 Paul Kessler, James Johnson. NASA Strategy and Architecture Office (SAO) Lunar Architecture Team (LAT). Aug 21, 2024. NASA: Evolution to Sustainable Lunar Habitation – Fall 2024 Project. Retrieved from: https://ntrs.nasa.gov/api/citations/20240010692/downloads/Evolution%20to%20Sustainable%20Habitation%202024.pdf .

3 Zheng Chen, Lixin Zhang, Yunchao Tang and Ben Chen. Pioneering lunar habitats through comparative analysis of in-situ concrete technologies: A critical review. Construction and Building Materials. Vol. 435, 12 July 2024, 136833.

Retrieved from: https://doi.org/10.1016/j.conbuildmat.2024.136833. and, https://www.sciencedirect.com/science/article/abs/pii/S0950061824019755.

4 Crawford, I. A. Lunar Resources: A Review. Progress in Physical Geography Earth and Environment. . (2015). 39(2), 137–167. DI: 10.1177/0309133314567585. https://doi.org/10.48550/arXiv.1410.6865

5 Gerald B Sanders, William E. Larson. Progress Made in Lunar In-Situ Resource Utilization under NASA's Exploration Technology and Development Program. Journal of Aerospace Engineering. April 2012 , 26(1). DOI: 10.1061/9780784412190.050. https://www.researchgate.net/publication/260321341_Progress_Made_in_Lunar_In-Situ_Resource_Utilization_under_NASA's_Exploration_Technology_and_Development_Program.

6. Kristine Ferrone, CharlesWillis, Fada Guan , Jingfei Ma , Leif Peterson and Stephen Kry. A Review of Magnetic Shielding Technology for Space Radiation. Radiation 2023, 3, 46–57. https://doi.org/10.3390/radiation3010005; Retrieved from: https://www.mdpi.com/journal/radiation

7. S.A. Washburn, S.R. Blattnig, R.C. Singleterry, S.C. Westover. Active magnetic radiation shielding system analysis and key technologies. Life Sciences in Space Research. Volume 4,January 2015, Pages 22-34. https://www.doi.org/10.1016/j.lssr.2014.12.004 .

8. Ramon Ferreiro Garcia. Power Plants and Cycles: Advances and trends. Book (2020): ISBN: 9789390431595; DOI:10.9734/bpi/mono/978-93-90431-59-5. https://www.researchgate.net/publication/347635047_Power_Plants_and_Cycles_Advances_and_Trends

9. Ramon Ferreiro Garcia, Jose Carbia Carril. Combined Cycle Consisting of Closed Processes Based Cycle Powered by A Reversible Heat Pump that Exceed Carnot Factor. Journal of Advances in Physics, Volume 15, (2018), Pages: 6078-6100. ISSN: 2347-3487. DOI: 10.24297/jap.v15i0.8034.

10. Ramon Ferreiro Garcia. Study of the disruptive design of a thermal power plant implemented by several power units coupled in cascade. Energy Technol. 2023, 2300362 (1-17). Published by Wiley-VCH GmbH. DOI: https://doi.org/10.1002/ente.202300362.

11. Ramón Ferreiro Garcia. Efficient disruptive power plant-based heat engines doing work by means of strictly isothermal closed processes. Journal of Advances in Physics Vol 22 (2024), p 30.53, ISSN: 2347-3487. https://rajpub.com/index.php/jap/article/view/9587. DOI: https://doi.org/10.24297/jap.v15i0.9587.

12. Ramón Ferreiro Garcia. Design study of a disruptive self-powered power plant prototype. *JOURNAL OF ADVANCES IN PHYSICS*, Vol 22 (2024), p 62.92, ISSN: 2347-3487. https://rajpub.com/index.php/jap/article/view/9596. DOI: https://doi.org/10.24297/jap.v22i.9596.

13. Ramón Ferreiro Garcia. Prototyping a Disruptive Self-Sustaining Power Plant enabled to overcome Perpetual Motion Machines. *JOURNAL OF ADVANCES IN PHYSICS*, Vol. 22 (2024), p 141.178, ISSN: 2347-3487. https://rajpub.com/index.php/jap/article/view/963. DOI: https://doi.org/10.24297/jap.v22i.9633.

14. Ramón Ferreiro Garcia. Prototyping Self-Sustaining Power Machines with Cascaded Power Units Composed by Pulse Gas Turbines. *JOURNAL OF ADVANCES IN PHYSICS*, Vol. 22 (2024), p 141.178, ISSN: 2347-3487. https://rajpub.com/index.php/jap/article/view/9648. DOI: https://doi.org/10.24297/jap.v22i.9648

15. E. W. Lemmon, M. L. Huber, M. O. McLinden, NIST Reference Fluid Thermodynamic And Transport Properties - REFPROP Version 8.0, User's Guide, NIST, Boulder, CO. 2007.

16. Ramón Ferreiro Garcia. Prototyping disruptive self-sufficiency power machines composed by cascaded power units based on thermo-hydraulic actuators. *JOURNAL OF ADVANCES IN PHYSICS*, Vol 22 (2024), p 141.178, ISSN: 2347-3487. https://rajpub.com/index.php/jap/article/view/9662. DOI: https://doi.org/10.24297/jap.v22i.9662.

17. Ramón Ferreiro Garcia. How to violate the first law of thermodynamics with an ASE of Papain and Newcomen before it was stated by Clausius. *JOURNAL OF ADVANCES IN PHYSICS*, *23*, 9–27. (2025) https://doi.org/10.24297/jap.v23i.9706

18. Ramón Ferreiro Garcia. Self-Sustaining Power Machines enabled to operate without both heat sink and heat source. *JOURNAL OF ADVANCES IN PHYSICS*, Vol. *23*,. (2025) pi–pf ISSN: 2347-3487https://doi.org/10.24297/jap.v23i.9727

19. Ferreiro Garcia, R. (2025). Preliminary design tasks for prototyping Self Sustaining Power Machines on Mars using local resources. .*JOURNAL OF ADVANCES IN PHYSICS*, *23*, 83–115. https://doi.org/10.24297/jap.v23i.9737. Retrieved from:

https://www.researchgate.net/publication/392326433_Preliminary_design_tasks_for_prototyping_Self_Sustaining_Power_Machines_on_Mars_using_local_resources

20. Patent: Planta térmica con máquina de doble efecto, acumuladores térmicos, convección forzada y alimentación térmica reforzada con un ciclo Brayton inverso y procedimiento de operación. Thermal power plant with double-effect machine, thermal accumulators, forced convection and reinforced thermal supply with a reverse Brayton cycle and operating procedure. Ramon Ferreiro Garcia, Jose Carbia Carril. application number 201700667 and publication number 2 696 950 B2. Accessed at: https://consultas2.oepm.es/ceo/jsp/busqueda/busqRapida.xhtml;jsessionid=MDkG1OIa9BfQrxSiImwxtYlC.ConsultasC2.

21. Patent: Procedimiento de operación de una máquina alternativa de doble efecto con adición y extracción de calor y convección forzada. Operating procedure of a double-acting reciprocating machine with heat addition and extraction and forced convection and operating procedure. Jose Carbia Carril, Ramon Ferreiro Garcia, application number P201700718 and publication number 2 704 449 B2. Accessed at: https://consultas2.oepm.es/ceo/jsp/busqueda/busqRapida.xhtml;jsessionid=-wHy58sbfVYQutIYN8s0+JKK.ConsultasC1.

22. Patent: Planta termoeléctrica multiestructural policíclica y procedimientos de operación. Polycyclic multi-structure thermal power plant and operating procedures. Ramon Ferreiro Garcia, application number P202200035 and publication number 2 956 342 B2. Accessed at: https://consultas2.oepm.es/ceo/jsp/busqueda/busqRapida.xhtml;jsessionid=-wHy58sbfVYQutIYN8s0+JKK.ConsultasC1.